

Research Paper

Centrifuge modelling of landslides and landslide hazard mitigation: A review

Kun Fang ^a, Huiming Tang ^{a,b,*}, Changdong Li ^{a,b}, Xuexue Su ^a, Pengju An ^a, Sixuan Sun ^a^a Faculty of Engineering, China University of Geosciences, Wuhan 430074, China^b Badong National Observation and Research Station of Geohazards, China University of Geosciences, Wuhan 430074, China

ARTICLE INFO

Article history:

Received 6 April 2022

Revised 6 September 2022

Accepted 10 October 2022

Available online 17 October 2022

Handling Editor: W.G. Zhang

Keywords:

Centrifuge test

Landslide

Slope stability

Scaling law

Mitigation strategy

ABSTRACT

Landslides are serious geohazards that occur under a variety of climatic conditions and can cause many casualties and significant economic losses. Centrifuge modelling, as a representative type of physical modelling, provides a realistic simulation of the stress level in a small-scale model and has been applied over the last 50 years to develop a better understanding of landslides. With recent developments in this technology, the application of centrifuge modelling in landslide science has significantly increased. Here, we present an overview of physical models that can capture landslide processes during centrifuge modelling. This review focuses on (i) the experimental principles and considerations, (ii) landslide models subjected to various triggering factors, including centrifugal acceleration, rainfall, earthquakes, water level changes, thawing permafrost, excavation, external loading and miscellaneous conditions, and (iii) different methods for mitigating landslides modelled in centrifuge, such as the application of nails, piles, geotextiles, vegetation, etc. The behaviors of all the centrifuge models are discussed, with emphasis on the deformation and failure mechanisms and experimental techniques. Based on this review, we provide a best-practice methodology for preparing a centrifuge landslide test and propose further efforts in terms of the seven aspects of model materials, testing design and equipment, measurement methods, scaling laws, full-scale test applications, landslide early warning, and 3D modelling to better understand the complex behaviour of landslides.

© 2022 China University of Geosciences (Beijing) and Peking University. Published by Elsevier B.V. on behalf of China University of Geosciences (Beijing). This is an open access article under the CC BY-NC-ND license (<http://creativecommons.org/licenses/by-nc-nd/4.0/>).

1. Introduction

1.1. Centrifuge modelling in landslide science

Landslides occur worldwide in diverse terranes and under a wide variety of climatic conditions. Catastrophic examples have disastrous, long-term societal impacts, including fatalities, significant economic losses, destruction of homes and buildings, disruption of transportation and utility infrastructures, and negative environmental effects (Highland and Bobrowsky, 2008).

The cause of a landslide is any factor that reduces the safety factor from a stable state to a situation that is actively unstable. The multitude of causes include geological, morphological, and human causes, which normally develop following only one trigger (Cruden and Varnes, 1996). In landslide science, heavy rainfall,

earthquakes, changes in water levels, rapid snowmelt, volcanic eruptions, and human activities are the most common landslide triggers (Wieczorek, 1996; Zhang et al., 2018b; Yao et al., 2020). To improve the slope stability and lessen the associated hazards, reducing driving forces and increasing resisting forces are two stabilisation categories used to increase the slope stability. According to these two routes and landslides subjected to different triggers, the methods for landslide mitigation at a site are diverse, including unloading, drainage, reinforcement, and vegetation. Owing to the complexity, scope and destructiveness of landslides, a comprehensive understanding of the behaviour of landslides subjected to each trigger and effective methods for preventing or mitigating their risks is needed.

A landslide is defined as “a physical system that develops in time through stages of prefailure deformation, failure itself and postfailure displacement” (Leroueil, 2001). In landslide science, the methods of investigating engineering problems related to landslides and hazard mitigation can be divided into reality-based methods, such as field investigations and basic laboratory tests, conceptual models (theoretical analysis), and physical or numerical modelling (Fig. 1).

* Corresponding author at: Faculty of Engineering, China University of Geosciences, Wuhan 430074, China.

E-mail addresses: kunfang@cug.edu.cn (K. Fang), tanghm@cug.edu.cn, hmtang6205@sina.com, tanghm@cug.edu.cn (H. Tang).

Physical modelling is a common and useful approach employed in landslide science that provides experimental data for the validation of numerical models and can reveal the mechanisms of slope deformation or failure at a site. Prefailure landslide deformation is called slope deformation in physical models. Failure or postfailure displacement of the landslide is considered slope failure during testing. The different methods for physical modelling of landslides can be categorized into the following three basic types: 1g small-scale physical modelling (e.g., Wang and Sassa, 2003; Lee et al., 2011; Zhu et al., 2020; Ivanov et al., 2021; Fang et al., 2022b), 1g large-scale or full-scale physical modelling (e.g., Moriwaki et al., 2004; Springman et al., 2012; Maghsoudloo et al., 2021; Zhang et al., 2021), and centrifuge modelling (e.g., Take et al., 2004; Ng et al., 2016b; Huang and Zhang, 2020; Wang et al., 2021).

Centrifuge modelling is an experimental method that has been applied in landslide science to simulate geological processes. The advantage of centrifuge modelling is that the individual effects of different parameters on landslides can be investigated by using simplified boundaries and geometries in an artificially high field of gravity. Furthermore, the progressive processes of the geohazard from beginning to end, which are difficult to comprehensively observe at sites, can be easily interpreted from photographs captured during the modelling process. The landslide processes in a desired environment can be controlled at a shorter length scale (decimetres to metres) and time scale (minutes to hours) than those observed in nature. Additionally, this method offers three-dimensional (3D) observations of the behaviours of landslides with large strain and can provide new insights into these hazards.

1.2. Literature review

Numerous research articles on centrifuge modelling of landslides have been published in academic journals and proceedings. A total of 660 articles on centrifuge modelling of landslides have been published in the landslide field from 1985 to 2019, with an increase in the number of articles published from 1 in 1988 to 102 in 2018 (Fig. 2). The development of the research papers on this topic can be mainly divided into three stages. In the first period from 1988 to 1996, fewer than ten research works were published per year, for a total of 25. The limited number of articles

in this period indicates that research regarding centrifuge modelling for landslides was lacking due to the poor practicability of the technology that was in a few laboratories. As the number of centrifuge laboratories gradually increased, the number of published articles in the second stage of research, which was from 1997 to 2014, experienced a small rise and fluctuation, with an average of 20 papers published per year. With the development of mature technology and wide recognition, centrifuge modelling has flourished in the landslide field in the third stage, which spans from 2015 to today. Generally, landslide studies using centrifuge models have experienced rapid growth.

The keyword frequency and representative articles usually reflect the hot topics and research interests within a certain field. In the existing research articles, the most popular keywords are “centrifuge tests” and “modelling slope” (Fig. 3). By emphasizing the details of centrifuge modelling for landslides, the frequently used terms are identified. The keywords “study”, “analysis”, “method”, “soil slope”, and “flow” signify the implementation of a centrifuge landslide test. The terms “failure”, “stability”, “mechanism”, and “deformation” are related to the deformation and failure behaviour of a landslide model. The keywords “pile”, “geosynthetics”, and “reinforced” are linked to effective stabilisation methods for landslide mitigation. A top ten list of high citation publications in the field is shown in Fig. 4. Like the top keywords, deformation or failure behaviour, mitigation methods, and centrifuge measurement in centrifuge landslide models are the main topics of the top ten papers.

The list of research institutions and countries shows the areas that focus on the research on this topic and suffer from landslide hazards. Fig. 5 contains the bibliometric results of centrifuge modelling of landslides by country. China leads the research and has performed extensive studies, with 25.8% of all articles originating from China; this is because China has the highest incidence of natural hazards in the world. The United States, Japan, and the United Kingdom follow behind China in terms of publications. Landslide research involving the centrifuge technique has been largely conducted at institutions equipped with centrifuge machines. Table 1 and Fig. 6 show that centrifuge landslide tests have been conducted at institutions all over the world. Centrifuge tests are being used to simulate landslides at more than 50 different laboratories. More than half of the facilities are in China, Japan, the United States and the United Kingdom, which allows for landslide tests to be conducted and many publications to be produced. Here, most of the centrifuges used in landslide research are quite large, typically with radii of 1 m to 3 m, but the two largest centrifuges have radii of 7.0 m and 9.1 m and are in Japan and the United States, respectively.

Furthermore, Fig. 7 shows the research categories of the publications using centrifuge modelling for landslides. Engineering geological and geosciences multidisciplinary are the most involved fields, accounting for 74% of all articles, and 16% of the articles are in the multidisciplinary field of engineering civil and material science. The remaining fields mainly include engineering environmental, environmental science, engineering mechanical.

1.3. Contents of the review

In the last 50 years, with the increase and development of centrifuge centres, instrumentation and actuation, an increasing number of centrifuge slope tests have been carried out. Based on the scientific literature survey above, in this paper, our goal is to offer complete state-of-the-art centrifuge modelling of landslides for students, engineers and scholars, with an emphasis on conducting centrifuge landslide testing. We provide a detailed review of the centrifuge slope tests used to ascertain landslide behaviors under various conditions and to determine effective methods for their mitigation.

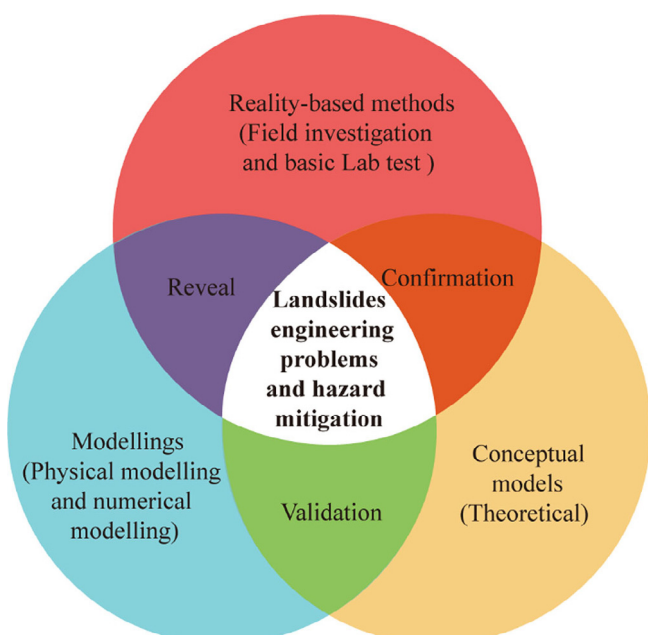


Fig. 1. Methods for investigating landslide engineering problems and hazard mitigation.

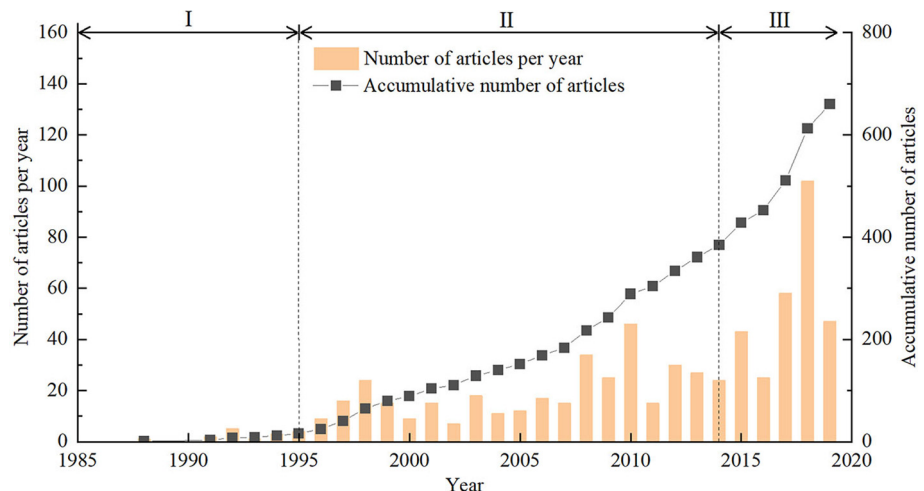


Fig. 2. Number of articles on centrifuge modelling of landslides since 1985 (from the online database Web of Science accessed on 9 Oct 2020: <https://apps.webofknowledge.com/>). Search topic = ["centrifuge landslide" or "centrifuge slope"].

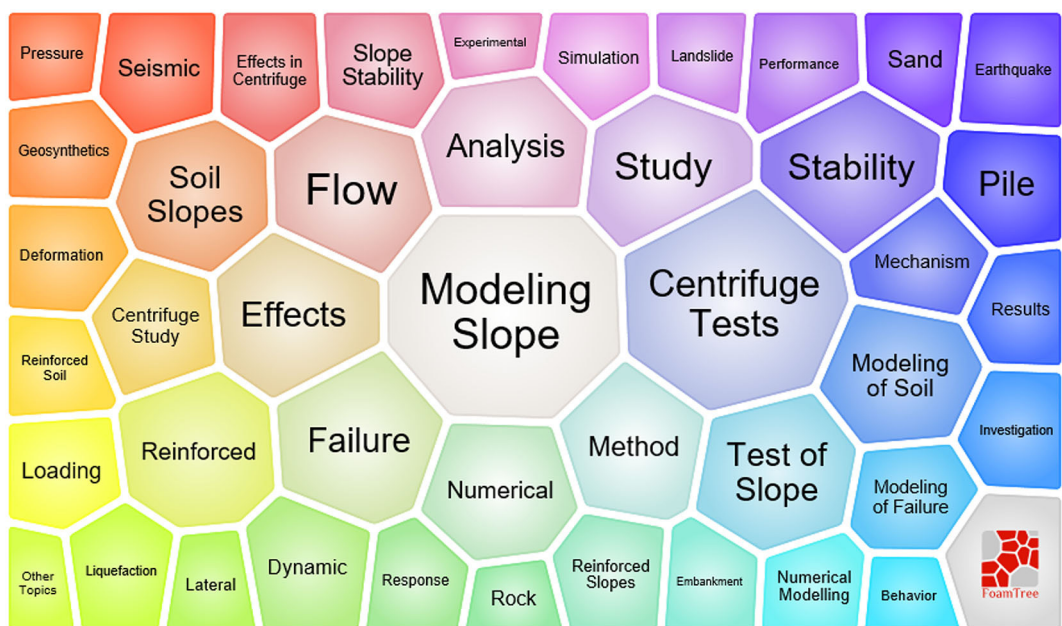


Fig. 3. Frequently used keywords in the articles related to centrifuge modelling of landslides (from the software Carrot2: <https://github.com/carrot2/carrot2>).

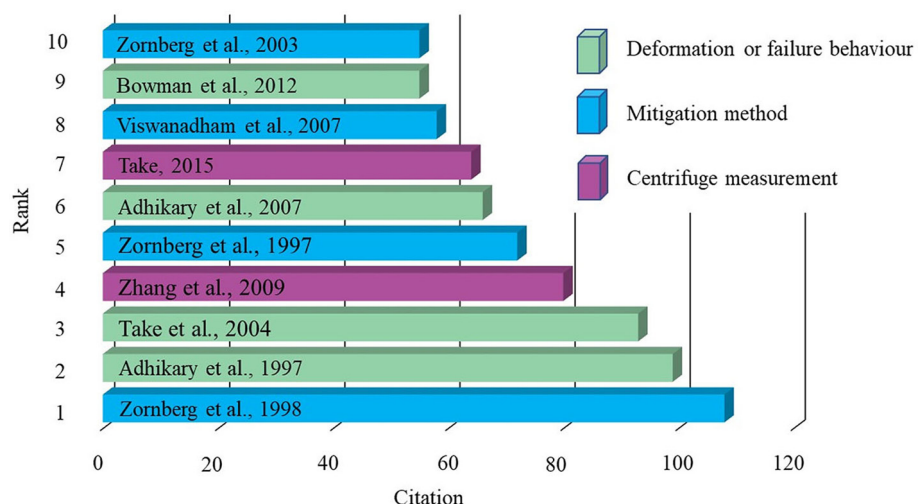


Fig. 4. Ten most cited articles in the field of centrifuge landslide modelling (from the online database Web of Science accessed on 9 Oct 2020).

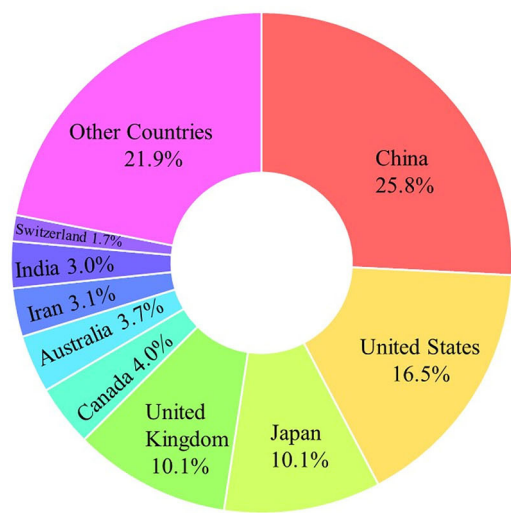


Fig. 5. Top countries using centrifuge modelling for landslides (from the online database Web of Science accessed on 9 Oct 2020).

Section 2 describes the principles of centrifuge modelling and landslide model consideration. Then, the characteristics of landslides induced by centrifugal acceleration, rainfall, earthquakes, water level changes, permafrost thawing, excavation, external loading, and miscellaneous conditions under high acceleration are summarized in Section 3, with a focus on deformation and failure mechanisms. Landslide mitigation at the centrifuge scale is presented in Section 4, with an emphasis on the use of nails, piles, geotextiles, vegetation, and other mitigation methods. Finally, we propose some recommendations for centrifuge modelling of landslides based on the reviewed studies in Section 5 and Section 6.

Table 1
Institutions that have performed centrifuge tests on landslides.

Institution	Country ^a	Radius (m)	Cap ^c (g·t)	Institution	Country ^a	Radius (m)	Cap ^c (g·t)
Changsha UST	China	3.5	150	U of Manchester	UK	3.2	600
Chengdu U of Tech	China	4.5	500	U of Nottingham	UK	2	50
CRSRI	China	3.7	200	U of Sheffield	UK	2	50
Dalian U of Tech	China	0.7 ^b	–	UMIST	UK	1.5	100
Hong Kong UST	China	4.2	400	Columbia U	US	3	300
IWHR	China	5.03	450	RPI	US	3	100
Nat Cent U, Taiwan	China	3	32	U of California, Davis	US	9.1	1080
NHRI	China	2	60	U of Colorado Boulder	US	1.36	15
Southwest Jiaotong U	China	3	100	U of Maryland	US	1.5	15
Tongji U	China	3	150	UENF	Brazil	1.7	100
Tsinghua U	China	2	250	UENF	Brazil	0.5 ^b	90
Zhejiang U	China	4.5	400	UWA	Australia	1.8	40
Gunma U	Japan	0.35	1	UWA	Australia	0.6 ^b	290
JNIOSH	Japan	2.3	50	Bandung Inst of Tech	Indonesia	1.8	–
Kajima Co	Japan	2.47	100	BOKU	Austria	1.31	10
Kyoto U	Japan	2.5	24	C-CORE	Canada	5.5	–
Kyusyu Inst of Tech	Japan	1.27	27	Delft TU	Netherlands	1.3	–
Nippon Koei Co	Japan	2.6	250	ETH Zurich	Switzerland	1.1 ^b	880
NNGI	Japan	2.7	100	Indian Inst of Tech	India	4.5	250
Obayashi Co	Japan	7.01	700	ISMGEO	Italy	2	240
PARI	Japan	3.8	312	K-water Inst	South Korea	5	240
Public Works Res Inst	Japan	6.6	400	LCPC	France	5.5	200
Shimizu Co	Japan	3.35	75	Iran U of Sci and Tech	Iran	1	14
Tokyo Inst of Tech	Japan	2.2	50	Nat U of Singapore	Singapore	2	40
Cambridge U	UK	4.13	150	Russian U of Trans	Russia	2.5	–
Cambridge U	UK	0.5 ^b	–	ULA	Colombia	1.7	40
Cardiff U	UK	2.8	100	U of Pretoria	South Africa	3	150
U of Dundee	UK	3.5	130				

^a from the website of the United Nations (<https://www.un.org/en/member-states>).

^b drum centrifuge.

^c maximum capacity.

2. Principles and experimental considerations of centrifuge modelling for landslides

2.1. Principles

The principles and essential features of centrifuge modelling involve replicating the prototype slope behaviour within a small model by increasing the acceleration from 1g condition to ng , which provides identical stress and strain in the model and the prototype at corresponding points. Figs. 8 and 9 show the slope model under high acceleration fields in a drum centrifuge and a beam centrifuge, respectively. According to the centrifugal acceleration ng in the model, the general scaling laws used in centrifuge modelling for landslides and reinforced materials are shown in Table 2. The most important advantage of a geotechnical centrifuge is that the stress state of the prototype can be properly replicated. The correct contractive-dilative behaviour can be modelled in a reduced-scale model (Ng, 2014). Despite some limitations in centrifuge modelling, such as nonuniform stress in slope models due to acceleration differences, particle size effects, and Coriolis effects, these shortcomings can be appropriately overcome through detailed preparations or special designs.

The objectives of centrifuge modelling for landslides can be divided into three types: (i) Investigations of the deformation or failure mechanisms of landslides were mostly used. (ii) For the comparison between models and prototypes, the technique of “modelling of model” is also applied (Schofield 1980; Taylor 1995). Quantitative studies of centrifuge slope tests were also abundantly applied for validation. (iii) Only a few model tests for simulating a slope at a site were carried out due to the complex boundary conditions, stress histories, and loading paths.

Compared with 1g small-scale and full-scale physical modelling, there are four main advantages in using centrifuge modelling for landslides (see Table 3): (i) stresses and strains close to prototypes in the small centrifuge model can reproduce the land-

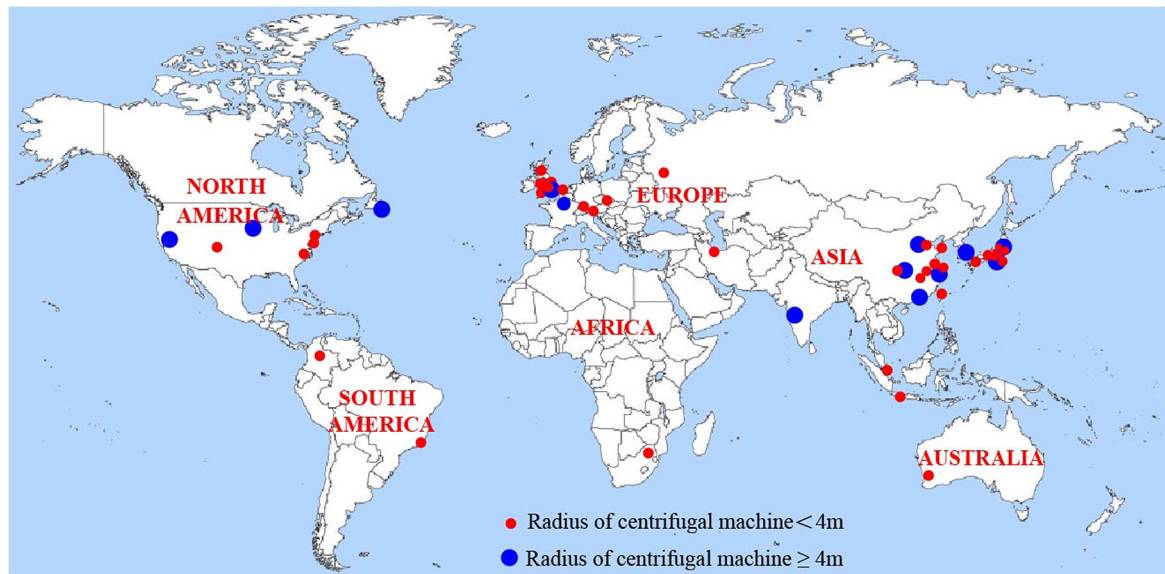


Fig. 6. Institutions that have conducted centrifuge landslide tests worldwide.

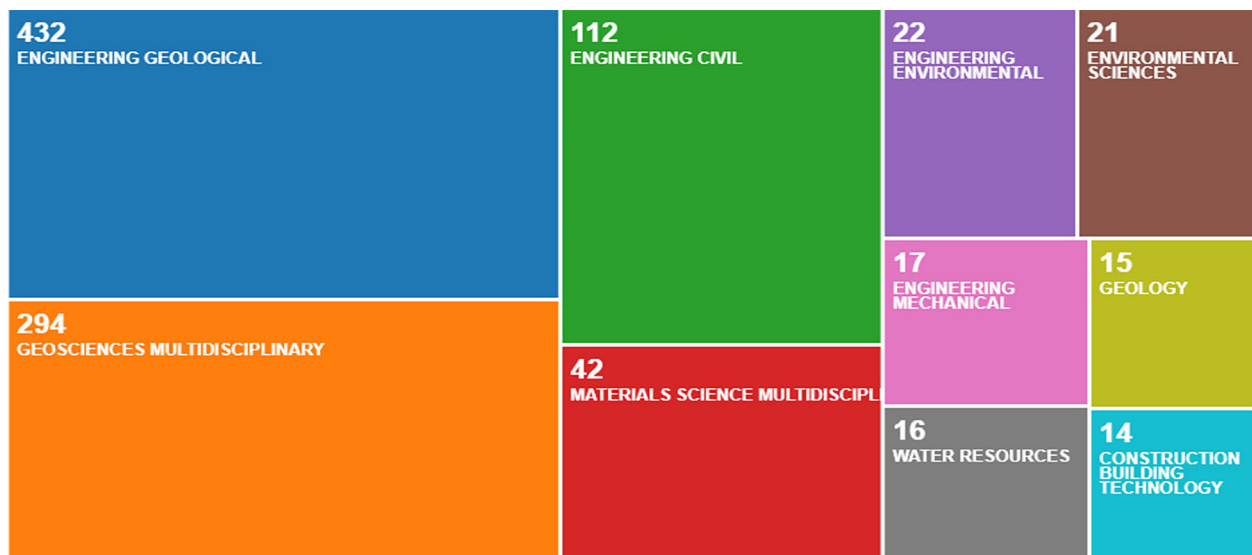


Fig. 7. Categories of research using centrifuge modelling for landslides (from the online database Web of Science accessed on 9 Oct 2020).

slide behaviours, which better reveals the deformation and failure mechanisms of a landslide; (ii) laboratory tests can greatly shorten the time scale needed to simulate natural processes, e.g., to model the long-term stress history of a clay slope or simulate a rainfall event on a slope model; (iii) centrifuge models can establish the feasibility of landslide recurrence under various triggers, including large earthquakes or thawing permafrost; and (iv) a smaller workforce and fewer experimental materials are required to prepare and construct a small-scale centrifuge model.

On the other hand, the limitation of centrifuge modelling must also be considered. Centrifuge modelling cannot simulate every geotechnical issue, such as issues related to structural failure and surface water flow.

2.2. Experimental considerations

2.2.1. Landslide model container

The designs of the containers for landslide models are different under drum centrifuges and beam centrifuges. In a drum cen-

trifuge, the drum is rotated around the whole edge of a cylinder that is spinning around its axis, as shown in Fig. 8. Beam centrifuges, made up of a rotating arm and swinging platform, are the majority of the centrifuges with longer radii, as shown in Table 1 and Fig. 9 (Kim et al., 2009; López et al., 2021). Based on the designs, sizes, and machine components of the two centrifuges, in a drum centrifuge test, the slope model is prepared inside the channel of the drum centrifuge (Morales Peñuela, 2013; Yin et al., 2019). In contrast, the slope containers used are rigid boxes or laminar boxes in a beam centrifuge test, depending on the objectives and requirements of the tests. For beam centrifugation, slope models are typically constructed in a rectangular rigid chamber with one transparent boundary under both static and dynamic conditions (Zhang et al., 2012; Higo et al., 2015; Miao et al., 2018; Pipatpongse et al., 2020). Although the back wall of a rigid container partly constrains the shear deformation of a slope model during shaking, constructing a long slope model is often adopted to weaken the effect of constrained deformation on all behaviours. Additionally, some dynamic centrifuge slope tests are conducted

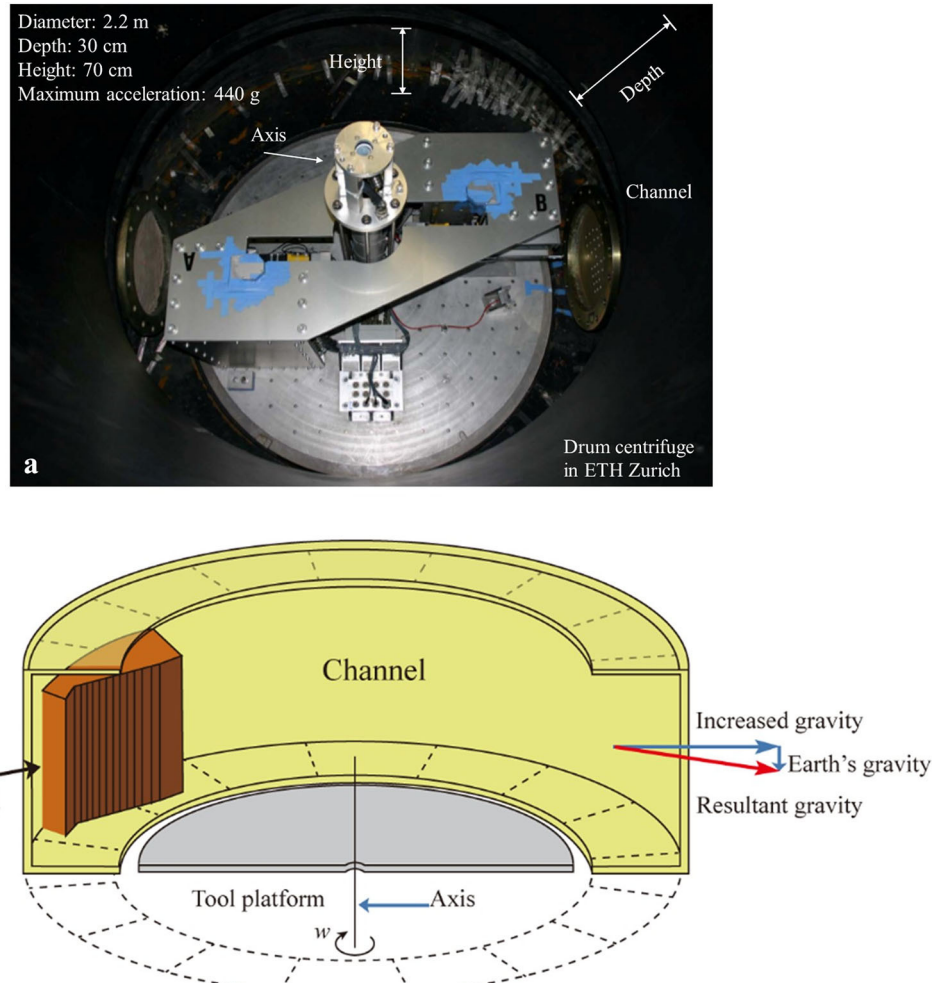


Fig. 8. Drum centrifuge: (a) drum centrifuge in ETH Zurich from a plan view; (b) schematic view of the drum centrifuge (modified from Morales, 2013, reuse with permission from Dr. Morales).

by using a laminar box that offers a semi-infinite horizontal boundary in the lateral direction (e.g., Liang and Knappett, 2017).

Centrifugal slope models are plane strain models in most cases. Due to two side frictions occurring between the slope and chamber, a wider container is suggested to decrease the proportion of the resistance force. Alternatively, lateral friction can also be reduced by using silicone oil (Wang et al., 2010b), a petroleum grease layer (Li et al., 2017), or rubber membrane sheets with grease (Ling et al., 2009).

2.2.2. Slope materials and model preparation

The tested materials play a major role in the deformation or failure behaviors of small-scale slope models. Ideally, the material particles in the slope centrifugal model are reduced in size by a factor n based on the scaling law. However, to maintain the same mechanical behaviors of the geomaterials in the prototype, the selection of materials, including particle sizes and physical properties, needs more consideration under high acceleration conditions. Fig. 10 shows some materials used for rock and soil slopes in centrifuge modelling. Soil slopes are usually modelled by using only soil or soil mixed with liquids (e.g., water and silicon oil in Tamate et al. (2012); saline water in Zhang et al. (2015c); water and glycerine solution in Askarinejad et al. (2015)). An elastic silica gel was recently used to simulate soil slope based on similarity law (Huang et al., 2020). The selections of materials for rock slopes in centrifugal tests are numerous due to the discontinuity properties

and failure types (see Fig. 10). The main materials used for rock slopes range from cement (e.g., Zhang et al., 2007; Zhen et al., 2013), gypsum (e.g., Adhikary et al. 1997), and plaster (e.g., Goldstein et al., 1966) to silica glass sheets (e.g., Adhikary and Dyskin 2007), alumina balls (e.g., Itoh et al., 2009b) and coal (Bowman et al., 2012). In addition, Tables 4–7 show model materials commonly used in reinforced slope tests. Aluminium materials are the commonly used items in nailed slope models (e.g., aluminium bars, tubes, and pipe) and piled slope models (e.g., aluminium tubes and cylinders), as shown in Tables 4 and 5. In geotextile reinforced slopes, polyester was widely applied (Zornberg et al., 1998; Hiro-oka et al., 2001) and new materials (e.g., hybrid geosynthetics) were also used in rainfall-induced slopes (Bhattacherjee and Viswanadham, 2019). Assorted vegetation models (e.g., acrylonitrile butadiene styrene plastic and fibre) and live vegetation (e.g., willow and avena sativa) have been used in vegetated slopes, as shown in Table 7.

In view of the selected materials, different preparation methods are applied. There are two main approaches to prepare soil slope models: tamping and pluviation. The unsaturated soil is normally compacted in layers to build a slope model with the required density using the tamping method. The pluviation method can be applied to dry soil slopes (e.g., Al-Defae and Knappett, 2014), unsaturated soil slopes (e.g., Take and Beddoe, 2014) and saturated soil slopes (e.g., Park and Kutter, 2015). On the other hand, the preparation of rock landslide models often includes a casting pro-

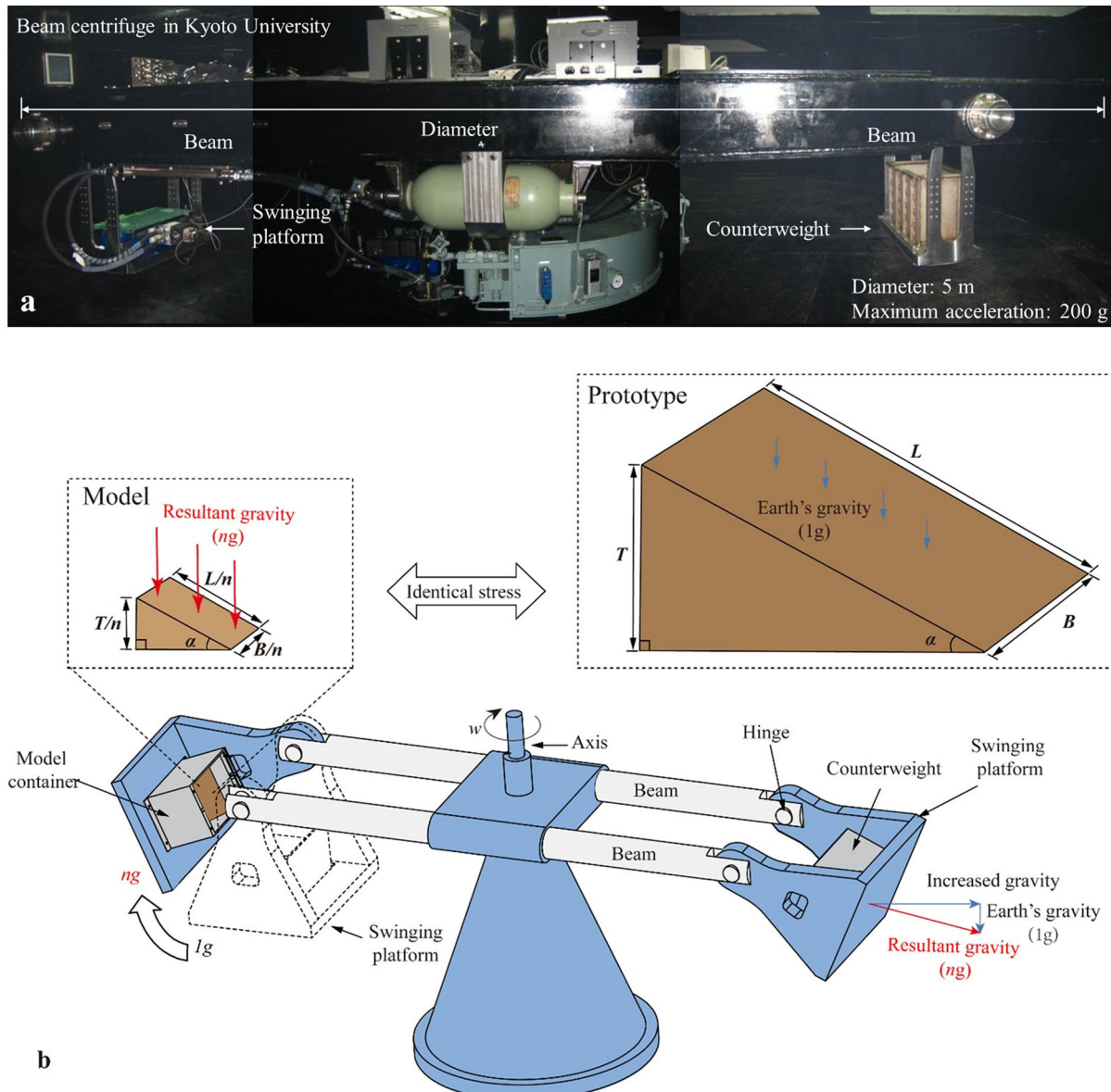


Fig. 9. Beam centrifuge: (a) beam centrifuge in Kyoto University from a plan view (modified from <https://sites.google.com/site/dpricentrifuge/home>, reuse with the permission from Assco. Prof. Kyohei Ueda); (b) schematic view of the beam centrifuge.

cess (e.g., Adhikary et al., 1997). To reproduce the performance of the prototype slope, the soil should possess the same fabric, structure, sensitivity, and stress history, as well as satisfy the same loading path, boundary stress state, and pore pressure distribution during the test. Meeting all these requirements is difficult, and some deviations from similitude appear to be inevitable.

3. Centrifuge modelling for landslides

Centrifuge modelling of landslides is summarized based on the following common landslide triggers: centrifugal acceleration, rainfall, earthquakes, water level changes, permafrost thawing, human activities (excavation and loading), and miscellaneous conditions, as shown in Fig. 11.

3.1. Centrifugal acceleration-induced landslides

It is generally known that the increased self-weight of the geomaterial in a model due to centrifugal acceleration by n times that

of Earth's gravity simulates the stress of the soil in a prototype. The increase in self-weight is considered to be an actuation in slope models. The deformations and failures of slope models are achieved by continuously increasing the rotation speed of the centrifuge machine. The applied gravity-induced body force in the slope is deemed to be a self-weight loading condition. In centrifuge modelling of landslides, the operation of self-weight loading starts from $1g$ and goes up to ng until failure occurs. Here, ng is the centrifugal acceleration at failure.

By increasing the centrifugal acceleration, the process of self-weight loading can be simply called g-up in this context; thus, a centrifuge test for a gravity-induced landslide is named a g-up test. It is also called a "gravity turn-on" test.

3.1.1. Soil landslides

Early researchers (e.g., Smith and Hobbs, 1974; Goodings and Schofield, 1985) carried out a series of g-up tests and compared the results with the limit analysis, finite-element method and limit equilibrium analysis (LEA), which gave self-consistent results in

Table 2

Centrifuge scaling laws related to landslides (modified from Schofield 1980; Taylor 1995).

Condition	Parameter	Unit	Model	Prototype	Condition	Parameter	Unit	Model	Prototype
All conditions	Length/Height	m	1/N	1	Rainfall and water level changes	Amount of rainfall	m	1/N	1
	Area	m^2	$1/N^2$	1		Duration of rainfall	s	$1/N^2$	1
	Volume	m^3	$1/N^3$	1		Time (seepage)	s	$1/N^2$	
	Velocity	m/s	1	1		Rainfall intensity	m/s	N	1
	Angle of friction	°	1	1		Hydraulic conductivity/Coefficient of permeability	m/s	N	1
	Cohesion	Pa	1	1		Seepage velocity	m/s	N	1
	Stress/Pressure	Pa	1	1		Water flow rate	m^3/s	$1/N$	1
	Elastic/Shear modulus	Pa	1	1					
	Force	N	$1/N^2$	1		Impact pressure on slope	Pa	1	1
	Mass	kg	$1/N^3$	1		Pore water pressure	Pa	1	1
	Mass density	kg/m^3	1	1		Suction	Pa	1	1
	Displacement	m	$1/N$	1		Hydraulic gradient	–	1	1
	Strain	–	1	1		Viscosity coefficient ^a	Pa·s	1	1
Dynamic condition	Time (dynamic)	s	$1/N$	1	Reinforced materials	Tensile strength	Pa	1	1
	Time (consolidation)	s	$1/N^2$	1		Axial rigidity	$Pa \cdot m^2$	$1/N^2$	1
	Frequency	Hz	N	1		Flexural rigidity	$Pa \cdot m^4$	$1/N^4$	1
	Acceleration	m/s^2	N	1		Pullout resistance	N	$1/N^2$	1
	Strain rate	s^{-1}	N	1		Moment	$N \cdot m$	$1/N^3$	1
	Shear wave velocity	m/s	1	1		Stiffness	N/m	$1/N$	1
	Energy	J	$1/N^3$	1		Second moment of inertia	m^4	$1/N^4$	1

Table 3

Comparison of the three physical model methods.

Condition	Centrifuge model	1g small-scale model	1g full-scale model
Stress intensity	★★★	★	★★
Test time	★	★★★	★★
Test preparation resource	★	★★	★★★
Test platform price	★★★	★	★★
Workforce for test	★	★★	★★★
Current operating frequency in landslide science	★★	★★★	★

The pentagram symbol represents the level or degree of the condition.

centrifuge modelling of landslides, as well as confidence in the development in engineering slope problems. The difficulty of simulating retrogression behaviour in a large-scale model was recognised because the loss of strength might be a function of unscaled displacement (Beasley, 1973) instead of strain (Mitchell, 1970; Goodings and Schofield, 1985). Later, g-up tests were mainly applied to ascertain the effects of the soil type (Ling et al., 2009; Zhang et al., 2015a), inclination (Ling et al., 2009; Zhang et al., 2015a; Idinger and Wu, 2019), degree of saturation (Idinger and Wu, 2019), bedrock (Zhao et al., 2018) and drainage layers (Hung et al., 2020) on the slope failure. During a g-up test, the shear zone reflecting the shear deformation localization was depicted by using the macroscopic measurement of the displacement, as shown in Fig. 12. A further contribution was made by Lü et al. (2019), who used a mixture of quartz sand, kaolin clay and peat to simulate municipal solid waste (MSW) slopes. The MSW slopes failed at 34.27g, and the slip surface consisted of a circular arc inside the slope and a straight line between the geomembrane and slope.

A few g-up tests have also been applied to cut slopes for short-term and long-term periods (Lyndon and Schofield, 1970). In these tests, after consolidation, the slope of the model was first cut under conditions of 1g. The slope model subsequently experienced a pre-set condition where the maximum centrifugal acceleration was less than the centrifugal failure acceleration. Finally, the time required to reach slope failure was recorded. Additionally, g-up tests using undisturbed soil samples were conducted in full-scale centrifugal modelling of the Lodalen landslide (Lyndon and

Schofield, 1978). The failure behaviours and time until failure in the model demonstrated an acceptable agreement with the prototype event, which showed the potential ability to solve the problems in situ.

3.1.2. Rock landslides

For rock landslides, the g-up test is the most widely used method in centrifuge modelling. Goldstein et al. (1966) conducted g-up tests to ascertain the stability of fissured rock slopes with different slope inclination angles (θ) and joint fall angles (δ). The three observed types of rupture surfaces were plane ($\delta > \phi'$), curvilinear ($\delta < \phi'$) and a combination of plane and cylindrical parts ($\delta > \theta$). Here, ϕ' is the angle of friction. The effects of the discontinuity and the key block in rock sliding failures were subsequently studied by Sugawara et al. (1983) and Zhen et al. (2013), respectively.

Toppling is a typical failure mode in rock landslides. By using the selected materials for the rock slope and discontinuity in centrifuge modelling (Fig. 10), three principal categories of toppling failure, namely, block toppling (Zhang et al., 2007), flexural toppling (Adhikary et al., 1997) and block-flexural toppling (Zhang et al., 2020a), were simulated in the g-up tests. Fig. 13 shows the three types of toppling failures in the tests. These experimental results were also compared with the limit equilibrium method and finite-element method. In addition, according to observations of the g-up tests of foliated rock slopes (Adhikary and Dyskin, 2007), the joint friction angle controlled the instantaneous and progressive flexural toppling failures.

3.2. Rainfall-induced landslides

3.2.1. Rainfall modelling

In designing a rainfall-induced slope model test, the following three main considerations regarding rainfall simulation should be noted: (i) uniform rainfall; (ii) rainfall droplets; and (iii) impact pressure. Rain simulators are significant in rainfall production and therefore influence the three concerns in centrifugal modelling mentioned above. Mist spray nozzles with injection pressure are generally used, as shown in Fig. 14. In addition, tests that apply a water outlet panel and spray water before spinning are successfully utilized.



Fig. 10. Typical geomaterials used in centrifuge modelling for landslides.

Table 4
Model nails in centrifuge slopes subjected to various triggers.

Triggering method	g	Model nail						Head or facing material	Slope material	Reference
		Material	d (mm) ^c	L/H ^d	S _H /H ^e	S _V /H ^f	θ (°) ^g			
g-up	–	Piano wire	–	0.85, 1.2	0.25	0.51	0	Thin grout layer	Silty sand	Shen et al. (1982)
Water level change	30	Stainless steel bar	1.7, 3	0.33–1.15	0.18	–	0, 10	Perspex	Sand	Tei et al. (1998)
g-up	–	Alu bars	2	0.32–1	0.12–0.16	–	10	Thin Alu sheet	Silty clay	Zhang et al. (2001)
Water level change	30	Alu tube	6.3 ^a	0.8	0.1	0.13	20	–	CDG soil	Zhou et al. (2006)
Water level change	30	Alu pipe	6.3	0.5, 0.83	0.21–0.25	0.17–0.25	15	Perspex sheet	Sand	Deepa and Viswanadham (2009)
Earthquake	50	Steel needles	0.8	0.29, 0.48	0.1, 0.19	0.1, 0.19	30	–	Sand	Wang et al. (2010a)
Water level change	30	Alu tube	6	0.83	0.29	0.29	10, 25	Alu plate and PoP ^b	Clean sand	Rotte and viswanadham (2013)
Earthquake	25	Brass screw bolt	3	0.35	0.24, 0.37	0.17, 0.33	25, 45	Alu plate	Sand	Nakamoto et al. (2017)

^a out diameter.

^b polyester fibre-blended plaster of Paris sheet.

^c nail diameter.

^d nail length/slope height.

^e horizontal nail spacing/slope height.

^f vertical nail spacing/slope height.

^g nail inclination measured from horizontal.

3.2.2. Rainfall-induced landslides in the centrifugal model

Seepage and pore water pressure (PWP) are two crucial factors in rainfall-induced landslides (Fredlund et al., 2012). There are two main failure mechanisms in these landslides regarding the PWP,

namely, positive and negative failure mechanisms (Collins and Znidarcic, 2004). In the positive mechanism, positive pressure located in the low area or near the bedding plane causes complete liquefaction of the failed mass. In the negative mechanism, suction

Table 5

Model piles in centrifuge slopes subjected to various conditions.

Triggering method	g	Model pile				Soil type	Reference
		Material	Diameter (mm)	Spacing ratio	Elastic modulus (GPa)		
Ground water level	50	–	–	0.125 ^c , 0.25 ^c	–	Sand	Takemura et al. (1994)
g-up	–	Aluminum tube	9.5	2.5–8.9	–	Sand	Yoon and Ellis (2009)
Earthquake	50	Aluminum tube	24.9×24.8 ^d	–	36	Sand	Yu et al. (2010)
Earthquake	40	Hollow steel	14×14 ^d	4.8, 7.1	210	Sand	Wang and Zhang (2014)
Earthquake	50	Concrete and Aluminum alloy	10×10 ^d	3.5–14	68 ^b	Sand	Al-Defae and Knappett (2014)
g-up and external loading	50 ^a	Aluminum and gypsum	17×17, 20×20 ^d	5	–	Silty clay	Zhang and Wang (2016)
g-up	–	Aluminum and acrylic tube	10	3.10–7.75	37.1, 3.1	Silty sand	Lei and Wu (2019)
External loading	50	Aluminum alloy cylinders	70	1.5	35	Sand	Di Laora and Fioravante (2018)
Earthquake	50	Aluminum tube with steel strand	26×36 ^d	3.5	70	Silica gel	Huang et al. (2020)

^a under the condition of external loading.^b Aluminum alloy pile.^c unit is pile/cm².^d rectangular intersecting surface.**Table 6**

Model geotextile reinforced slopes in centrifuge modelling.

Triggering method	g	Model geotextile				Soil type	Reference	
		Material	T _u (kN/m) ^a	ε _u (%) ^b	L/H ^c	S/H ^d		
g-up	–	PET ^f	0.05	18	0.5–0.75	0.13	Clay	Porbaha and goodings (1996)
g-up	–	PET ^f , PET with rayon	0.06, 0.12	–	0.89	0.06–0.19	Sand	Zornberg et al. (1998)
Water level change	50	PET ^f	0.27	13	1 ^h	0.17,0.33	SF ^e	Hiro-oka et al. (2001)
g-up, loading	–	Heat bonded fabric	5	–	1–1.3	0.25	Clay	Zimmie et al. (2005)
Earthquake	48,19.2	Pellon sheet	–	–	0.7, 0.9	–	Sand	Nova-Roessig and Sitar (2006)
g-up	–	Bandage gauze	3.15	7.78	0.22–0.83	0.14	Silty clay	Hu et al. (2010)
Rainfall	30	PET ^f + PVC + PP ^g	1.01, 2.08	18.3, 22.8	0.85	0.17	Sand	Bhattacherjee and Viswanadham (2019)

^a ultimate tensile strength.^b ultimate strain.^c geotextile length/slope height.^d geotextile spacing/slope height.^e very silty or clayed sand in British standard.^f polyester.^g polypropylene.^h obtained from figures.**Table 7**

Model vegetated slopes subjected to various conditions.

Triggering method	g	Vegetation	Geometry	RAR (%) ^a	Tensile strength (MPa)	Soil type	Reference
Water level change	15	Younger and older willow (live)	–	0.048	0.1, 16.1	Elastic silt	Sonnenberg et al. (2010)
Water level change	15	Wooden stick and rubber (model)	Straight and dichotomous	0.05, 0.18	85, 7.4	Sandy silt	Sonnenberg et al. (2012)
Rainfall, water level change	–	Fibre and sand (model)	–	–	–	Sand	Eab et al. (2015)
Rainfall	50	Avena Sativa (live)	–	0.01	–	Silty sand	Askarinejad and Springman (2015)
Rainfall	15	Cellulose acetate (model)	Tap, heart and plate shaped	0.1–0.75	31	CDG ^b soil	Ng et al. (2016)
Earthquake	10, 30	ABS ^c plastic (model)	Root cluster	–	–	Sand	Liang and Knappett (2017)
g-up	–	Lolium perenne, Hordeum vulgare and Festuca arundinacea (live)	–	–	–	Sand	Veenhof and Wu (2018)

^a root area ratio.^b completely decomposed granite.^c acrylonitrile butadiene styrene.

reduction results from rainfall infiltration in the unsaturated slope, and the slope finally fails with the decrease in shear strength.

Many centrifuge tests have been conducted on rainfall-induced landslides to study the negative mechanism. With the update of

the rainfall simulation using spray nozzles in the centrifugal atmospheric chamber (Kimura, 1991), a very loose unsaturated completely decomposed granite fill slope model test was carried out to assess the negative mechanism (Take et al., 2004). The PWP is

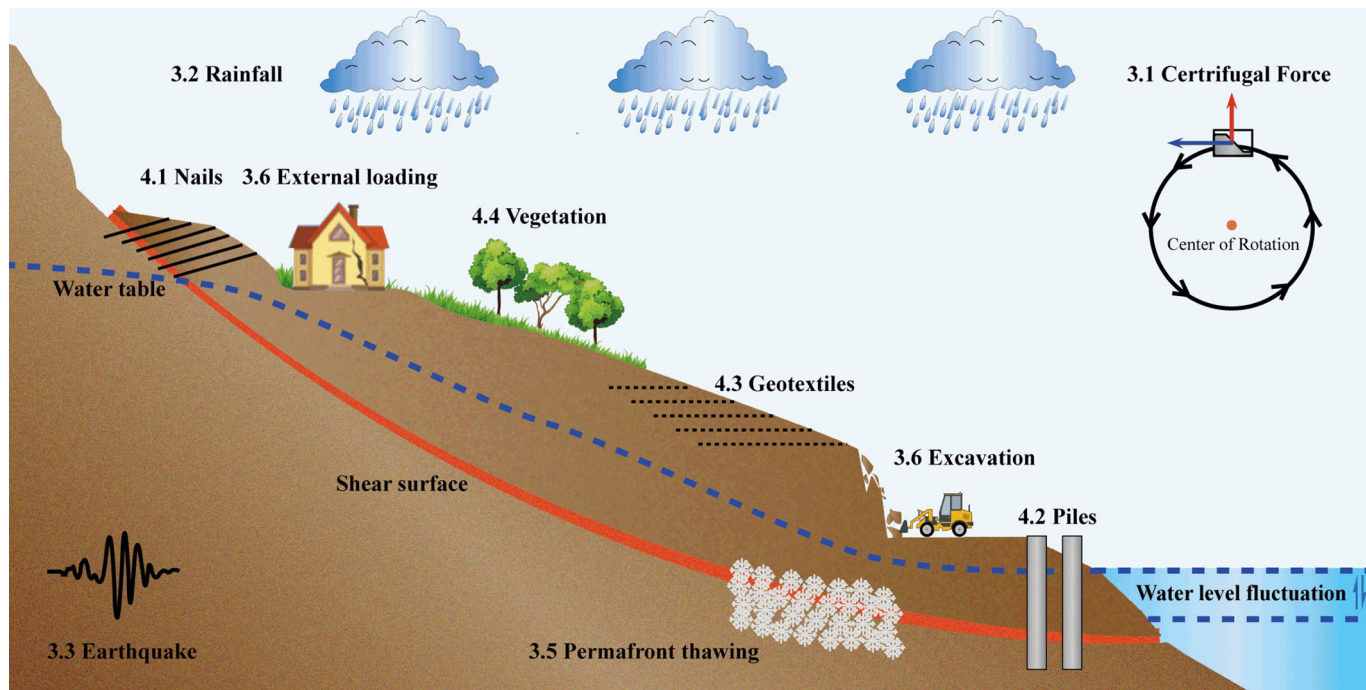


Fig. 11. Schematic figures of landslides subjected to various triggering factors in this study.

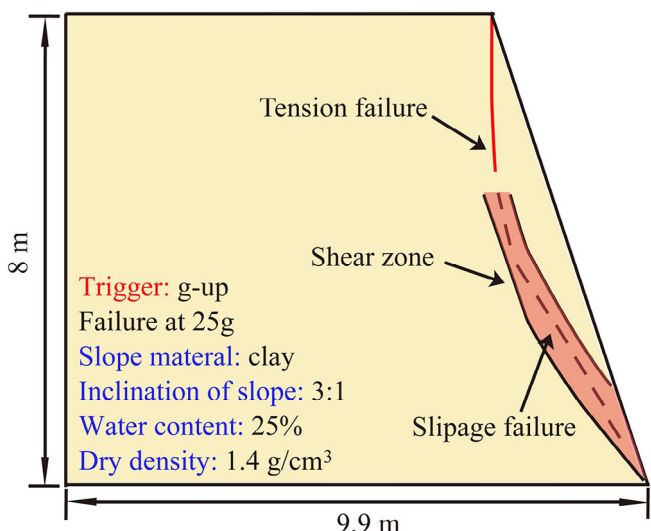


Fig. 12. Shear zone and slip surface in the slope model under g-up conditions (modified from Zhang et al., 2015a, reused with the permission of Springer Nature and Copyright Clearance Center).

approximately -25 kPa at the crest of the slope at 60g. However, it changes to a minimal negative value in the slope subjected to rainfall infiltration. The loss of suction causes a large downslope movement. Compared with the very loose slope test, Ling et al. (2009) conducted tests on sand-clay mixed slopes compacted under optimum conditions at both 60g and 80g and observed failures during large rainfall events (see Fig. 15). The safety factor decreases with the reduction in apparent cohesion, which is equivalent to the loss of matric suction. In addition, the effects of slope material (Cheng et al., 2011), weak layers (Wang et al., 2010b), and preexisting cracks (Zhang et al., 2012) in rainfall-induced slopes under negative mechanisms have also been reported.

The positive mechanism can be observed in rainfall-induced sand-clay slope models lying on bedrock (Ling and Ling, 2012). A

large positive PWP located at the toe near the bedding plane at 100g was recorded in a heavy rainfall simulation with a 200 mm rainfall increment, which indicates that flow may occur in these areas. At the critical moment, the PWP suddenly decreases due to deformation, resulting in a large global slide. This sudden change in PWP during rainfall was also observed at 50g in the first stage of failure for a 40-mm-thick loose slope on bedrock (Askarinejad et al., 2015), which resulted from void collapses. The dissipation of the excess PWP after rainfall subsequently caused the second-stage failure of the slope with the viscous solution. This failure mechanism in a very loose slope is also known as static liquefaction.

3.3. Earthquake-induced landslides

3.3.1. Earthquake modelling

Inspired by the development in hydraulic shakers, earthquake-induced landslides can be modelled in centrifugal tests by using a servo-hydraulic shaking table in flight, which generates multifrequency inputs and provides an opportunity to investigate the dynamic response of the slope model.

3.3.2. Earthquake-induced landslides in the centrifugal model

Various performances of centrifuge slope models are observed under seismic loading. One of the response behaviours is that accelerations at the base are amplified in the upper area of slopes. The amplification of the base accelerations due to the propagation of shear waves was monitored in embankment slopes with unsaturated soil (Kutter and James, 1989) and saturated soil (Ng et al., 2004). The acceleration response spectra curves were drawn to obtain the peak of the amplification factor and the corresponding frequency. In dry sand slopes subjected to earthquake loading, Yu et al. (2008) observed an amplification effect in the upper layer and on the slope surface. The amplification spectra at 5.7 Hz were the same as the natural frequency of the slope from the theory of resonance vibration. Brennan and Madabhushi (2009) reproduced the effect of amplification in a dry sand slope with a height H at

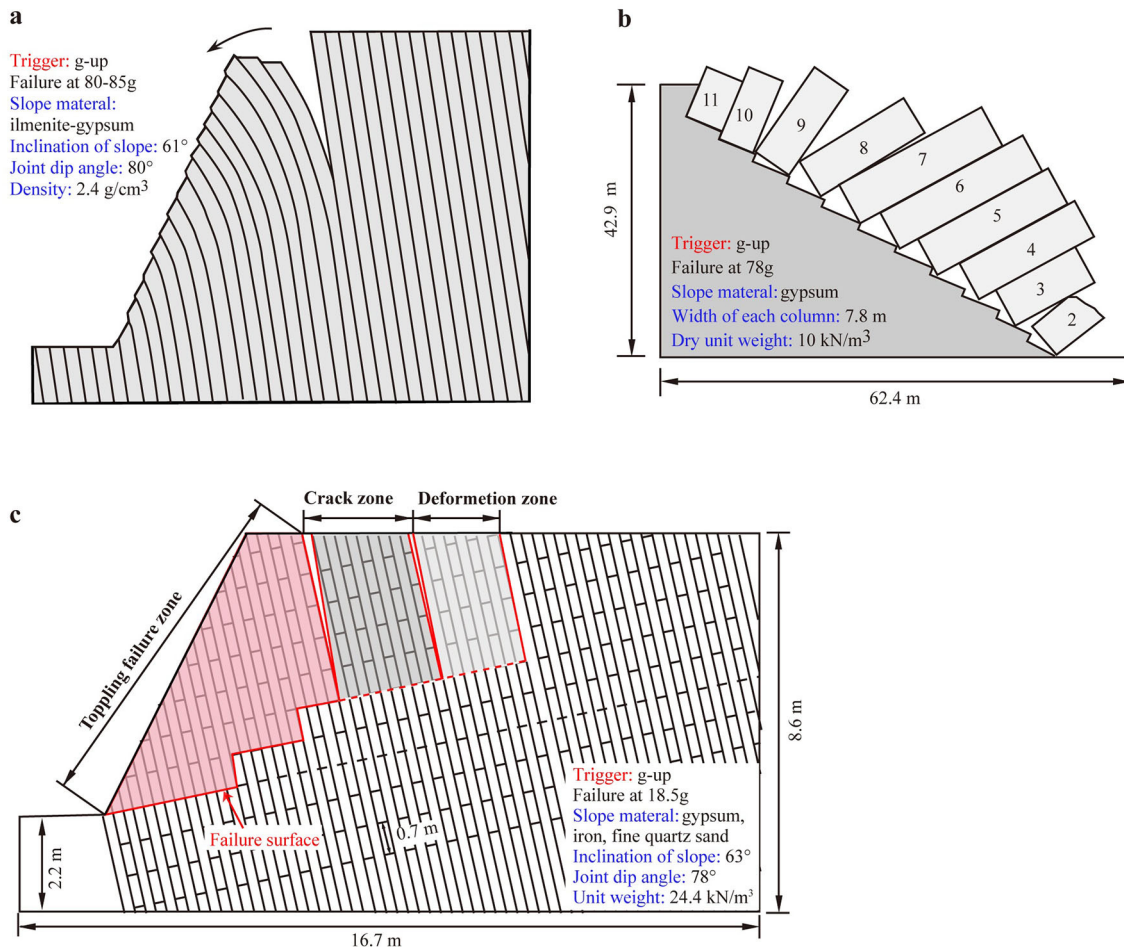


Fig. 13. Toppling failures in the slope models subjected to g-up: (a) flexural toppling (modified from Adhikary and Dyskin, 2007, reused with the permission of Springer Nature and Copyright Clearance Center); (b) block toppling (Zhang et al., 2007, reused with the permission of Springer Nature and Copyright Clearance Center); (c) block-flexure toppling (Zhang et al., 2020a, reused with the permission of Springer Nature and Copyright Clearance Center).

50g and the affected area was $0.63H$ and $0.31H$ deep at the crest. The presence of a gradient of acceleration from the ground to the crest results from the amplification. These slope amplification phenomena were also recorded in unsaturated loess slopes in both the horizontal and vertical directions (Zhang et al., 2017), a soil slope with a weak intercalated layer (Yan et al., 2019) and a rock-soil mixture deposit slope (Sun et al., 2019).

The behaviors of unsaturated and saturated slopes subjected to dynamic loading are different. In terms of unsaturated slopes, Matsuo et al. (2002) investigated earthquake-induced flowslides in unsaturated fills and infinite slopes. They observed and concluded that shear deformation mainly developed below the phreatic lines and near the toes of fill slopes. The degree of compaction, shaking intensity and elevation of flowslides determines the permanent deformation. On infinite slopes, flowslides occurred in slopes with low soil densities and large slope angles. The slide occurred at the discrete rupture zone instead of at the bottom of the slope due to the steady-state shear strength attained in the region. Once the flowslide was triggered, the slope displacement was independent of the shaking intensity. Enomoto and Sasaki (2015) also indicated that many factors affected the seismic behaviour of partially saturated slopes and mentioned that seepage water was the most crucial factor during the input shaking of the Hyogoken-Nambu earthquake in 1995. In addition, Higo et al. (2015) conducted dynamic tests of unsaturated embankment slopes constructed with various water contents. For the deforma-

tion behaviour of a slope with a higher than optimum water content, shear deformation with positive dilatancy was concentrated at the toe and beneath the slope surface, and shear deformation with large compression was located underneath the crest, resulting in subsidence of the crest.

On the other hand, liquefaction-induced landslides during earthquakes have been studied using centrifugal models of saturated slopes. An early study used saturated sand with a relative density of $D_r = 40\%$ to ascertain the dynamic response of the slope after initial liquefaction (Taboada-Urtuzuastegui et al., 2002). Under further shaking, an isolation behaviour of the horizontally layered sand located in the free field was observed due to the lack of shear stresses within the soils. In contrast, a dilative action in the slope area resulted in an increase in strength. A void redistribution in the liquefaction-induced slope deformation was subsequently considered (Kulasingam et al., 2004; Malwick et al., 2008). A typical centrifuge model for demonstrating the void redistribution mechanism consisted of a lower-permeability silt layer inside the sand slope, as shown in Fig. 16. According to 12 dynamic centrifuge slope model tests (Kulasingam et al., 2004), the strain localisation and associated deformations resulting from void redistribution were related to the initial relative density, the shape of the silt layer, the thickness of the sand layer and the shaking conditions. When sand slopes with an initial $D_r < 35\%$ were shaken for a long duration or slopes with a higher initial $D_r = 50\%$ were subjected to the strongest motion, localisation occurred. The mobilisation of the

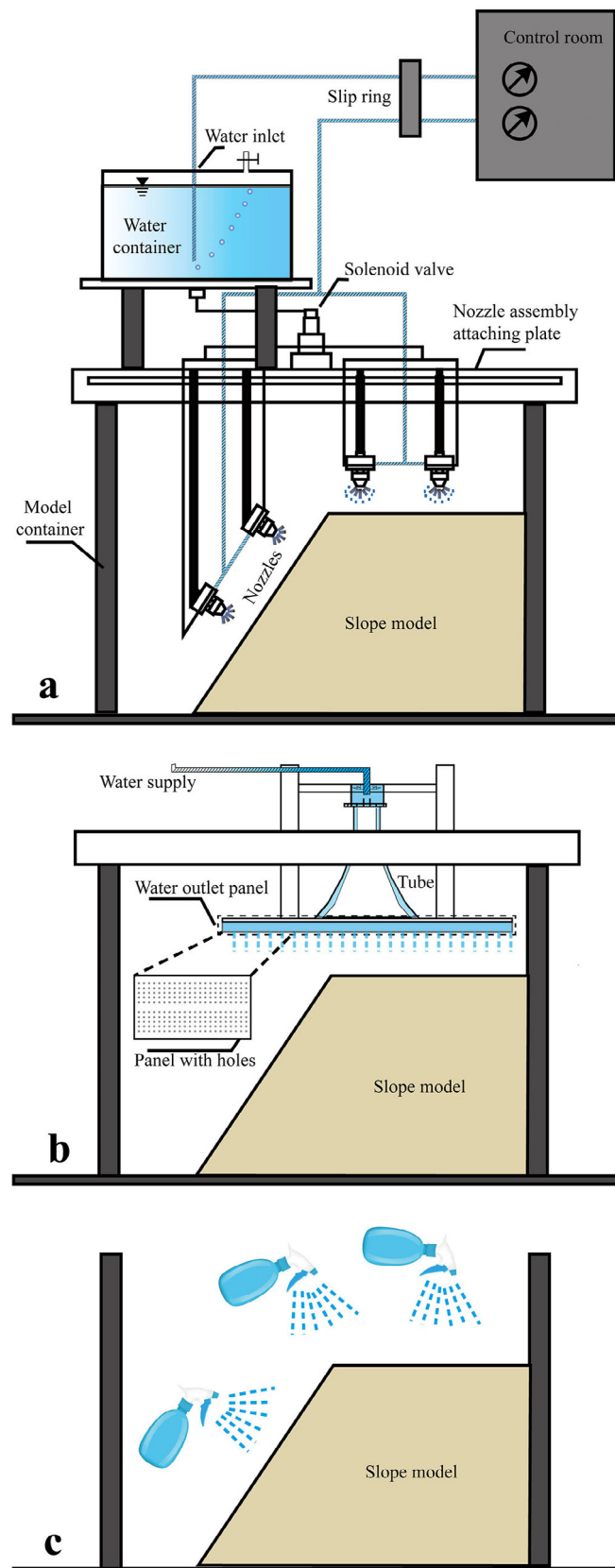


Fig. 14. Schematic figures of rainfall simulator in centrifuge landslide tests: (a) nozzles (modified from Bhattacherjee and Viswanadham, 2019, reused with the permission of American Society of Civil Engineers and Copyright Clearance Center); (b) water outlet panel (modified from Zhang and Wu, 2007, reuse with the permission from editorial office of Rock and Soil mechanis); (c) spraying water before spinning (Ling and Ling, 2012).

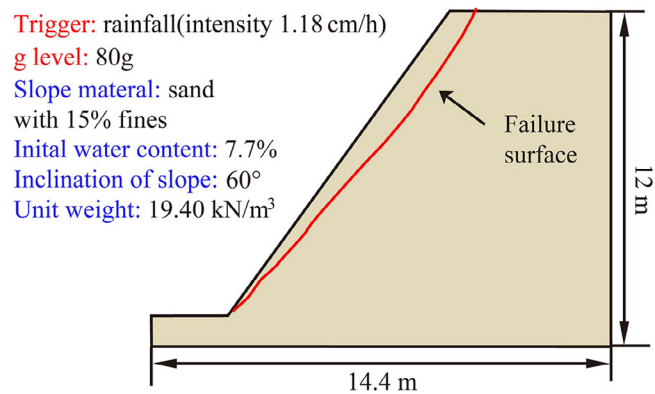


Fig. 15. Sliding failure of the slope model due to rainfall (modified from Ling et al., 2009, reused with the permission of American Society of Civil Engineers and Copyright Clearance Center).

shear resistance during the generation of high excess PWP also depends on all the factors mentioned above (Malvick et al., 2008). More recently, centrifuge tests of earthquake-induced slope failure have provided insights into sensitive clay slopes (Park and Kutter, 2015). In comparison to the distinct slip surface in static failure, multiple slip surfaces (diffused shear surface) contribute to a broader shear band in dynamic failure, as shown in Fig. 17. The shallow and deeper slip surfaces were also compared in static and dynamic failures, respectively. The sensitive clay slope was more stable than the insensitive clay slope due to the larger initial stiffness and insufficiently remoulded strain in the sensitive soil. Additionally, a debris flow was simulated in earthquake-induced submarine landslides with the aid of applied osmotic pressure from the ground (Takahashi et al., 2019). The Liquefaction Experiments and Analysis Projects (LEAP) focused on lateral spreading of the sloping ground considering gentle slopes (Kutter, 2020).

A few dynamic centrifuge tests have been carried out on the sliding failure and toppling failure of rock slopes, as well as MSW slopes (e.g., Thusyanthan et al., 2006; Li et al., 2015b).

3.4. Water level change

3.4.1. Modelling of water level changes

In the centrifuge models of landslides triggered by water level changes, the simulation of the water level change can be divided into ground water level (GWL) and reservoir water level (or river water level) fluctuations. The main difference between the two water levels is the location of the water supply during spinning (see Fig. 18). For a GWL change, water is normally applied at the top of a slope lying on a bedding plane or at the back of a slope to simulate the increase in the GWL inside slopes after prolonged precipitation. On the other hand, the supply and drainage water outside the slopes present the impounding and drawdown of a reservoir (or a river), respectively. For both conditions, the frequently used in-flight devices are composed of a water pump, water storage tank, water drainage tank, and control valves. Without a water pump, filling water before spinning and supplying water from a high elevation water storage tank were also used (Fang, 2019; Zhang et al., 2019a).

3.4.2. Landslides triggered by reservoir water level changes

Rapid drawdown eliminates the stabilising effect of water and causes higher shear stress due to resistance by undrained and drained strength within the slope (Duncan et al., 2014). The first discussion and analysis of a landslide triggered by a rapid drawdown in centrifuge modelling emerged in 1969 with the develop-

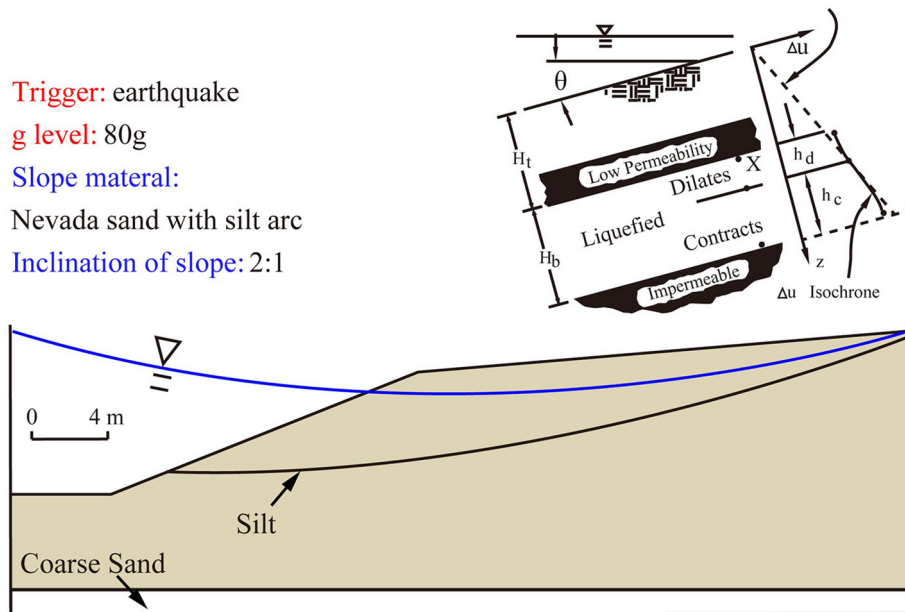


Fig. 16. Geometry of a slope subjected to an earthquake: (a) conceptual model; (b) centrifuge model (modified from Kulasingam et al., 2004, reused with the permission of American Society of Civil Engineers and Copyright Clearance Center).

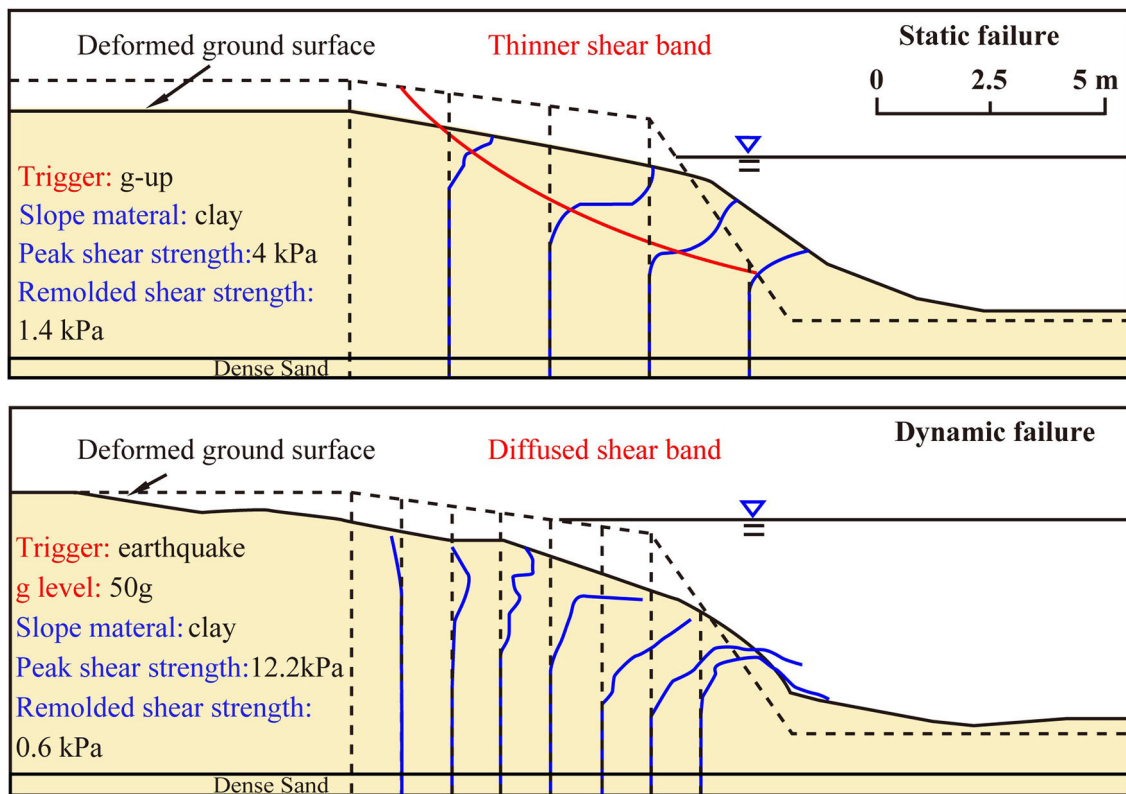


Fig. 17. A comparison of the shear band and shear strain in deformed slopes subjected to g-up and earthquakes (modified from Park and Kutter, 2015, reused with the permission of Elsevier and Copyright Clearance Center).

ment of centrifuge machines MK. I and MK. II at the University of Cambridge (Avgherinos and Schofield, 1969). The horizontal direction of the principal strain was near the toe, and the vertical strain was distributed at the middle and top. These internal strains also suggested a relationship between the remaining safety factor and displacement during the drawdown. Further study of the deforma-

tion behaviour of the slope during drawdown showed that a nearly invariable deformation zone associated with seepage in the slope was observed based on an image-based measurement at 50g (Luo and Zhang, 2016). For a slope on a nondeformable bedding plane subjected to multiple reservoir water level lowering events, the deformation mode was demonstrated at 80g in Fig. 19 (Li et al.,

2020). In addition, Li et al. (2015a) reported that the occurrence of the most considerable deformation was at the first water level fluctuation in a 100g test.

Retrogressive failure is frequently monitored in slope models subjected to water level fluctuations (Chen and Huang, 2011; Miao et al., 2018). The movement first occurs at the toe of the slope, sometimes accompanied by cracks, and subsequently causes the gradual failure in the middle and rear of the slope. Moreover, the effects of reservoir water level changes in the Xiaochatou landslide and Liangshuijiang landslide in the Three Gorges area, China, were studied in a centrifugal model to provide a better understanding to solve engineering problems (Fan et al., 2017; Miao et al., 2018).

3.4.3. Landslides triggered by GWL changes

An increase in the GWL due to prolonged rainfall or land irrigation allows groundwater to flow inside the slope, which reduces the shear strength with an increase in the degree of saturation and triggers landslides. Two types of centrifuge models involving GWL changes have been carried out. The first type consisted of trapezoidal-shaped slopes from the side view and a water supply system on the back of the slope. The second model simulated a slope lying on bedding rock by providing water at the crest of the slope.

A considerable amount of exploratory research on the GWL has been conducted for trapezoidal-shaped slopes. Takemura et al. (1994) performed centrifugal tests to ascertain the stability of trapezoidal-shaped slopes. Similar slope movements during pre-failure and deep sliding failure were confirmed in both the 25g centrifuge model and the 1g large-scale prototype model. Quick tests and slow tests were also compared by raising a water table with a height of 9 cm in 22 s and 170 s after reaching 50g. The slip surface and deformation area in the quick test were wider than those in the slow test due to the phreatic surface profile. The effect of GWL change patterns on the slope was addressed by Timpong et al. (2007). Additionally, the role of the rising GWL due to irrigation has been studied (Zhang et al., 2019a). The destruction of the structure of saturated loess due to the sharp increase in PWP resulted in the loss of strength. The detailed slope failure process is shown in Fig. 20. Moreover, a global slide with massive horizontal displacement, cracks and local slides was observed in a centrifugal MSW slope owing to the rising water level with a slope ratio of 1:1. The other failure modes were also captured and depended on the degradation state, slope gradient and reinforced berm (Chen et al., 2017).

The second type of experiment involving centrifuge modelling was demonstrated by Take et al. (2004). In their seminal experiments, a loose layered completely decomposed granite (CDG) slope acting on a bedding plane was tested at 30g by providing local ground water mounds at the top of the slope. The test supported an alternative hypothesis about the slide-to-flow transformation mechanism in fill slopes owing to groundwater ponding (Fig. 21). Rapid flow behaviour related to static liquefaction was observed due to the restriction of seepage water. In follow-up studies (Take and Beddoe, 2014; Take et al., 2015), with evidence of a dynamic pore pressure ratio monitored by the PWP pressure and shearing with no volume change observed by PIV analysis, static liquefaction failure was replicated in centrifuge model tests by gradually increasing the ground water flux. Based on the location of the shear-induced failure, the failure was called base liquefaction (Take and Beddoe, 2014). Compressible and sufficiently saturated soil subjected to monotonic loading facilitated the occurrence of base liquefaction. By combining the antecedent ground water conditions and rainfall, it was found that the mobility of a landslide, including the travel distance and velocity, was related to the preexisting GWL (Take et al., 2015). A higher preexisting GWL was prepared at 30g; more considerable travel distances and velocities were observed. Moreover, the effects of local heterogeneity (Lee et al., 2008), slope inclination (Beddoe and Take, 2015) and bedrock steps (Lucas et al., 2019) on the failure and mobility of landslides were also discussed. By gradually increasing the phreatic surface on a bedrock hillslope to 100g (Milne et al., 2012), the initiation of debris flow was modelled. Observation of the behaviour of sandier and siltier sands resisting the increasing PWP suggested that sandier soils were more likely to cause failure, which agreed with field monitoring in Scotland. Regarding the arching effect in the slope, the behaviour of the undercut slope subjected to increased ground water was carried out at 30g by Fang (2019), as shown in Fig. 22.

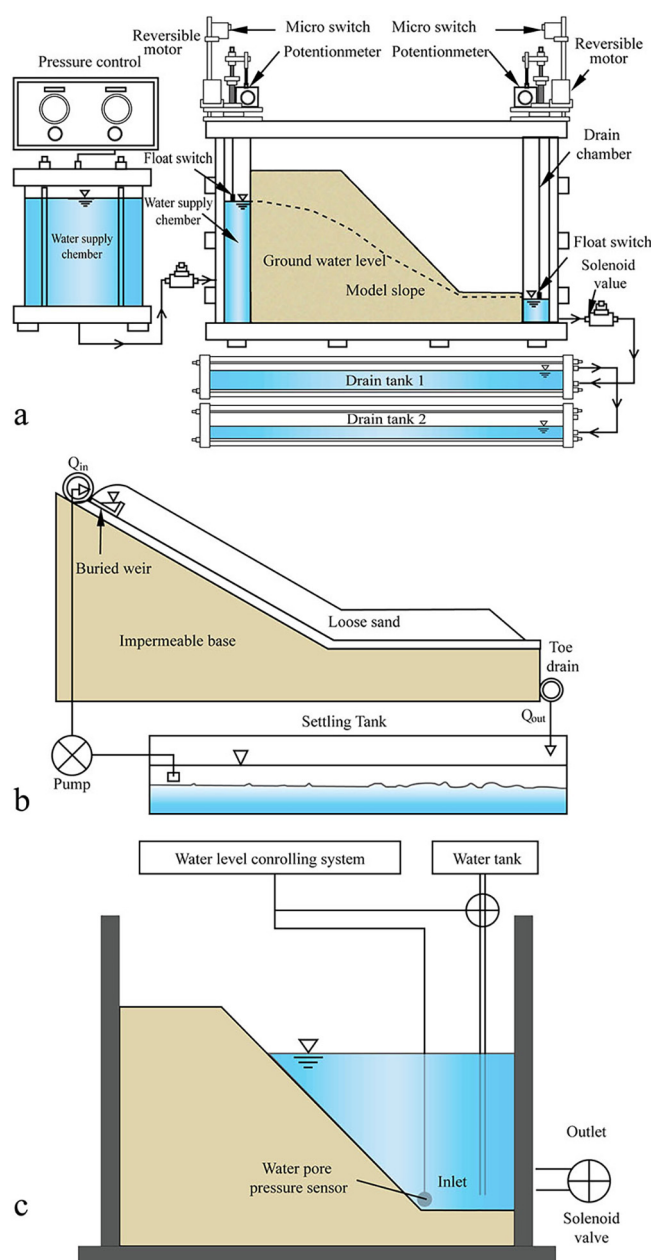


Fig. 18. Schematic figure of water supply in centrifuge landslide tests: (a) at the back of a slope model (modified from Timpong et al., 2007, reused with the permission from Prof. Kazuya Itoh); (b) at the top of a slope model (modified from Beddoe and Take et al., 2015, reused with the permission of Elsevier and Copyright Clearance Center); (c) outside a slope model (modified from Luo et al., 2018, reused with the permission of Elsevier and Copyright Clearance Center).

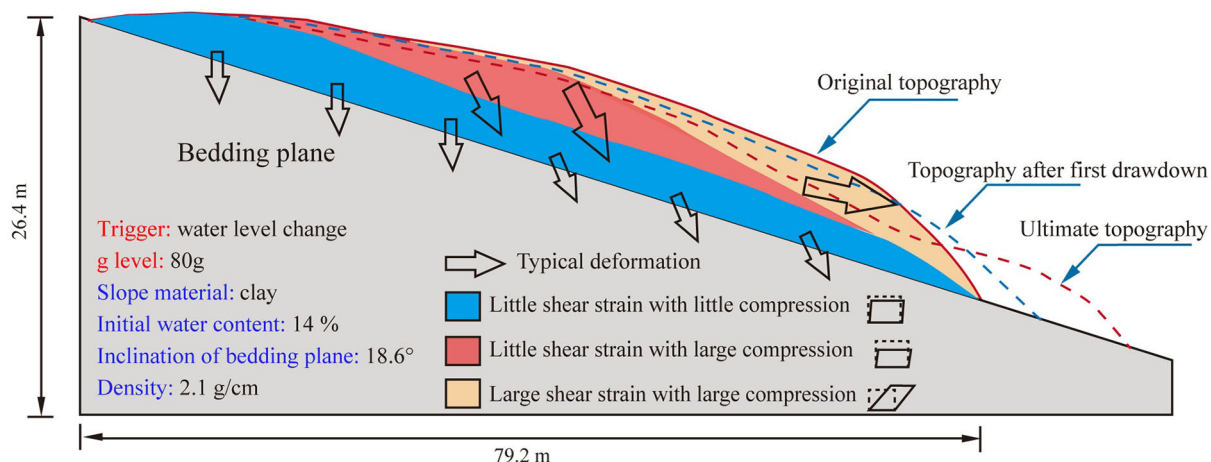


Fig. 19. Deformation mode of the landslide model subjected to a water level change (modified from Li et al., 2020, with permission from the MDPI publisher under a Creative Commons Attribution 4.0 International License (CC BY 4.0)).

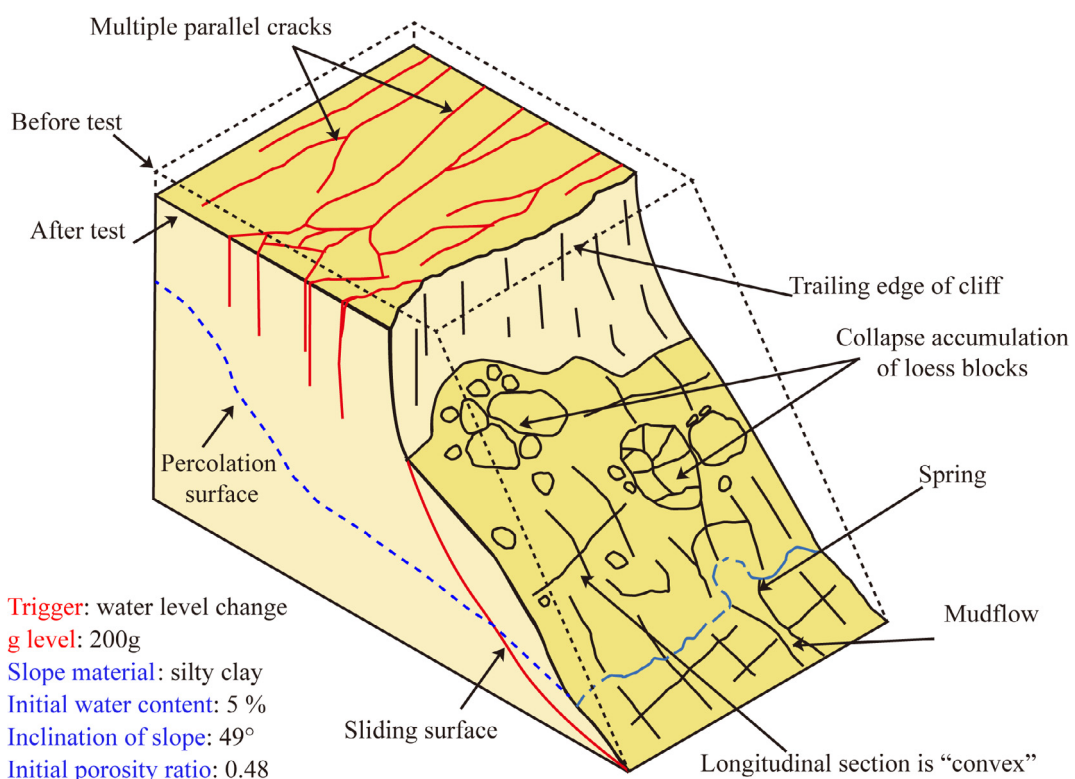


Fig. 20. Failure behaviours of the slope model subjected to a water level change (modified from Zhang et al., 2019a, reused with the permission of Elsevier and Copyright Clearance Center).

3.5. Permafrost thawing

Permafrost thawing and seasonal thawing in periglacial slopes cause prefailure solifluction. Early examples of centrifugal experiments on thawing slopes were demonstrated by Harris et al. (2001). The thawing process was achieved by directing a flow of warm air with a temperature of approximately 20 °C.

To ascertain the controversy regarding the solifluction behaviour, different scaled centrifuge tests at 10g and 30g were conducted in frozen models under freeze-thaw cycles (Harris et al., 2003). The behaviour was determined from monitoring the time of thaw and consolidation, as the different scaling laws for viscous

flow and elastoplastic soil were applied. The results showed that the soil mechanics approach was more appropriate in modelling prefailure shearing during the solifluction process. In systematic follow-up investigations (Harris et al., 2008), various mass movement processes, including mudflow, flowslides, solifluction and detachment slides, were clearly presented in centrifuge models with different clay contents and under different stress conditions (Fig. 23). Moreover, Davies et al. (2001) studied the impact of rising temperature on ice-filled rock slopes at 120g. They reported that a frozen slope at low temperatures was more stable than an unfrozen slope. However, when the ice in the rock discontinuities warmed, the slope became unstable.

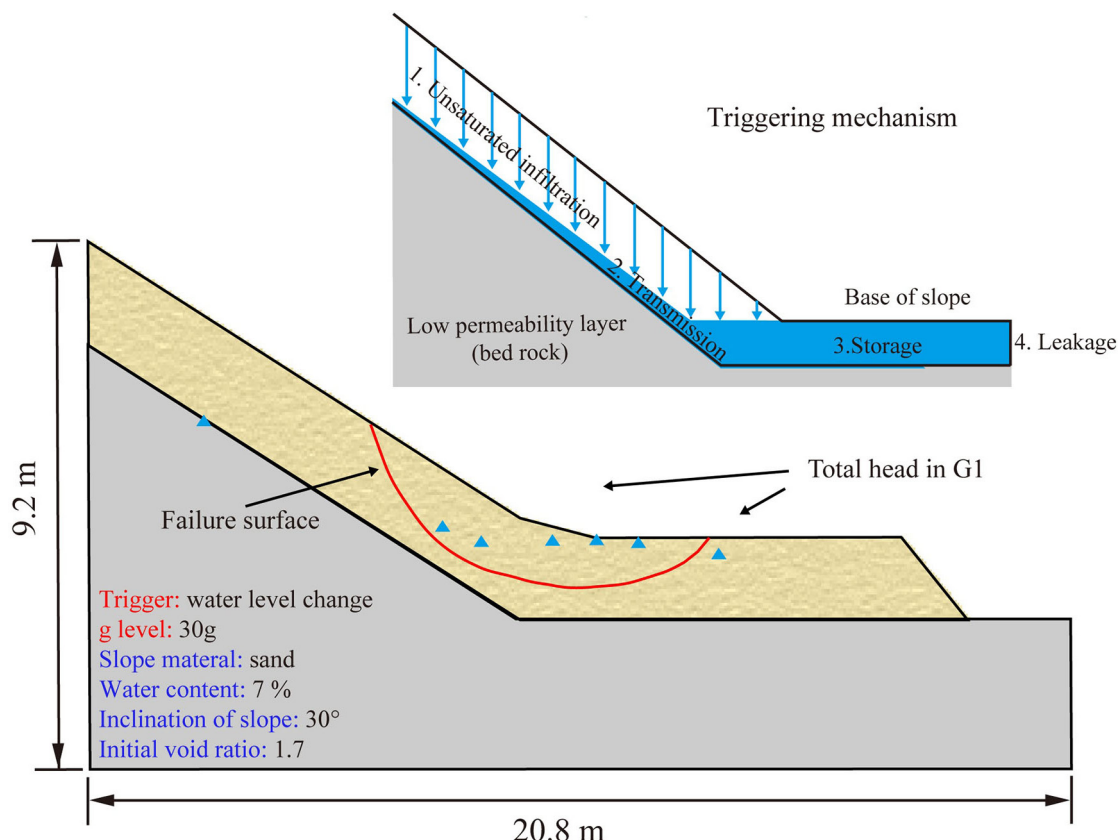


Fig. 21. Centrifuge test for demonstrating base liquefaction (modified from Take et al., 2015, reused with the permission of Springer Nature and Copyright Clearance Center).

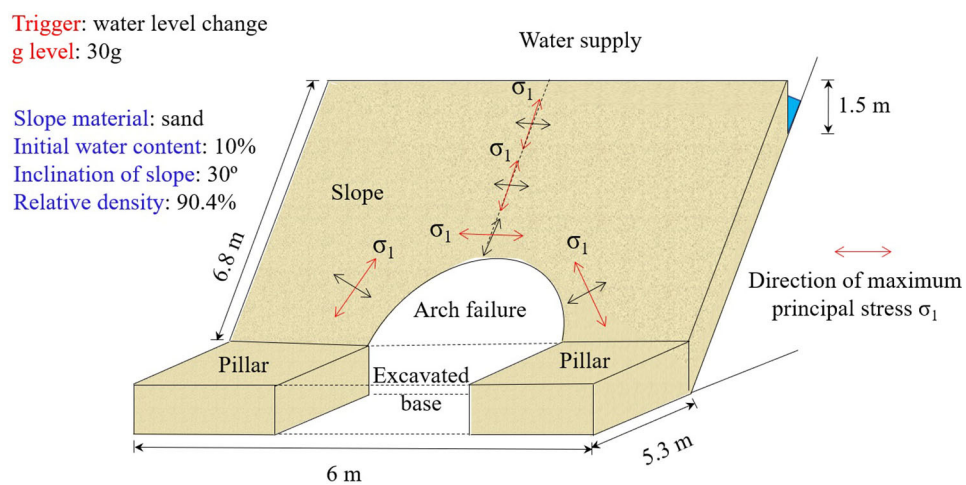


Fig. 22. Arch failure in a cut slope due to a water level change (modified from Fang, 2019).

3.6. Excavation and external loading

With the increasing demand for infrastructure, small landslides were reported and raised concerns during construction, such as excavation at the toe of a slope for road construction and external loading near the crest of a slope for building construction. Concerning the excavation process, Azevedo and Ko (1988) raised a soil bag with the aid of an electric motor to achieve the cutting process. A similar method was also applied in a rock slope excavation model by removing a plastic plate with a fixed pulley system at 80g (Li et al., 2016). In recent years, in-

flight excavation at the toe of a slope using a controlling system containing a motor and cutting blade has been widely used to investigate the effects of the soil properties (Tamrakar et al., 2006), slope inclination (Li et al., 2011), and excavation direction (Fan et al., 2016; Zhang et al., 2020b). The in-flight excavation method and the g-up pre-excavation technique in the same slope model were compared (Zhang et al., 2014). The results showed that the two methods representing two loading paths caused different stability levels and slip surfaces. To assess the arching effect in the slope during excavation, arch-shaped local failures with the formation of passive arch action were clearly observed

in a slope at 40g and in an undercut slope at 50g (Itoh et al., 2009a; Khosravi et al., 2016).

Unlike excavation models, few studies have examined the impact of static or cycling external loading on centrifuge slope models (Wang et al., 2018b). A deadweight surcharge dropped on the crest of the slope was used to trigger liquefaction (Phillips and Byrne, 1998), and a controlled pneumatic piston provided cycling loading on the top of an embankment slope to study the effect of train load (Vorster et al., 2017).

3.7. Miscellaneous conditions with various methods

3.7.1. Releasing gate method

A “releasing gate” is widely used to trigger landslides in centrifuge modelling. Using this technique, the flow behaviours of landslides, including rock falls, rock avalanches, dry flows, and flowslides, can be investigated. The releasing gate is also called the releasing door, releasing funnel, sliding door or triggering gate in the literature (Huang and Zhang, 2020; Zhang and Huang, 2022). Releasing gates are mainly applied to model the postfailure behaviour of a landslide, which means that the failure or collapse of the landslide has already occurred. The first centrifuge model for dry granular flows was designed by Vallejo et al. (2006). The deformation response and shearing resistance of the soil are stress dependent. However, centrifugal tests showed that fluid behaviour, not stress-dilatancy behaviour, was closer to the performance of dry granular flow (Bryant et al., 2015). Additionally, the flow depth and velocity values of released glass beads under different slope angles and centrifugal accelerations were also compared (Cabrera and Wu, 2017).

In addition to the dry flow, the reproduction of a dry rock fall and rock avalanche with centrifuge modelling has also attracted considerable interest. Itoh et al. (2009b) performed and observed four falling modes associated with fracturing, including free falling, bouncing, rolling and sliding, by using a rockfall generation system with a sliding door at 50g. Bowman et al. (2012) found that coal with a higher degree of fragmentation experienced a more extended runout in rock avalanches. Unsaturated soil and coal were also suitable materials to simulate the behaviours of debris flows and rock avalanches. According to a series of tests on debris

flows, flow volume and runout are dominated by fluid viscosity, water contents, and g-levels. All the observations of the debris flow behaviour in centrifuge modelling generally agreed with those of the 1g test. Regarding the runout of a cliff collapse, compared with the effect of block geometry and topography, the water content played a more important role in the resulting runout (Bowman and Take, 2015).

Over the past decade, research into submarine landslides has focused on centrifuge modelling. Early model tests of submarine flow in a drum centrifuge were conducted by releasing a sliding door or a stopper (Gue et al., 2010). During the movement of a debris flow on a 6° slope, the hydroplaning phenomenon was generated and depended on the water content and material properties (Acosta et al., 2017). The effects of the water content and shear properties on submarine debris flows were further investigated in hydroplaning and turbidity currents (Fig. 24) (Yin et al., 2019).

3.7.2. Tilting table method

Tilting table test, which is a load-control test that involves rotating the angle of a table, is applied to three aspects of centrifuge slope models, namely, pseudostatic loading imposed on the slope, toppling failure in the rock slope, and slope oversteepening effects on liquefaction. Khosravi et al. (2013) used a tilting table to apply a pseudostatic horizontal force to undercut slopes at 50g. The seismic stability of the slopes was analyzed with consideration of the pseudostatic seismic coefficient. By rotating the table at 30g, the toppling mechanism was studied in rock slopes consisting of aluminium and plastic cubic blocks. The zones of stability, toppling and sliding were observed, and the plastic block slope with bending resistance was more stable than the aluminium case (Chen et al., 2015). By using tilting techniques, the static liquefaction of both saturated submarine slopes and dry slopes was achieved (Wolinsky and Take, 2019; Zhang and Askarinejad, 2019). The slope instability regime was found to be controlled by the tilting velocity.

3.7.3. Heater method

Successive wetting and drying are important triggers for the deterioration and failure of slopes. To accelerate the drying process, the heater approach, which involves a lamp, heat bulbs and

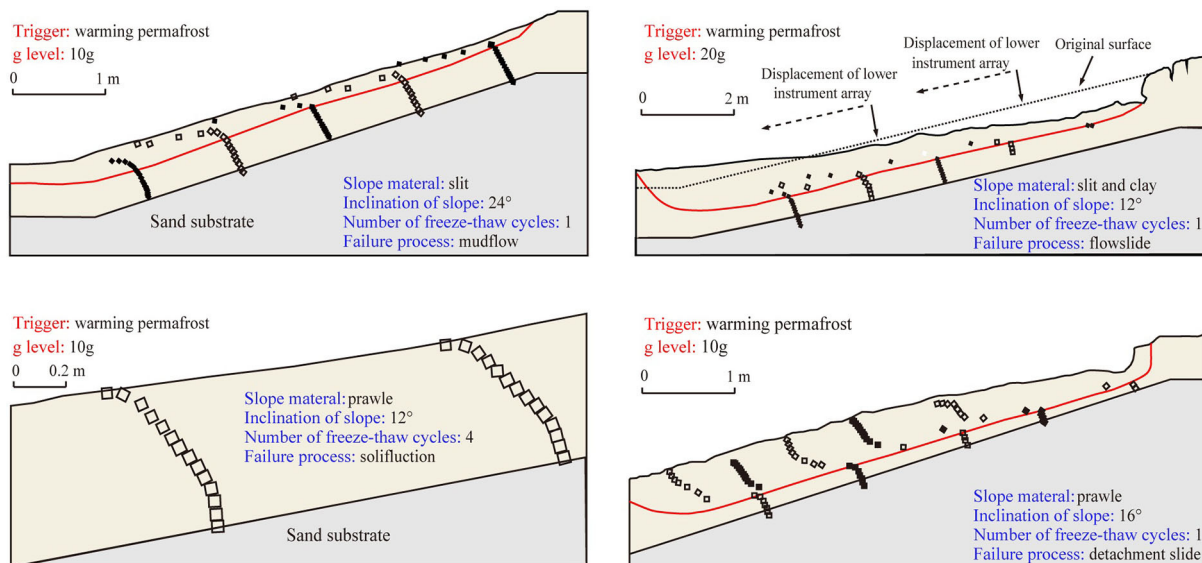


Fig. 23. Various failure processes associated with soil movement profiles under warming permafrost (modified from Harris et al., 2008, reused with the permission of Elsevier and Copyright Clearance Center).

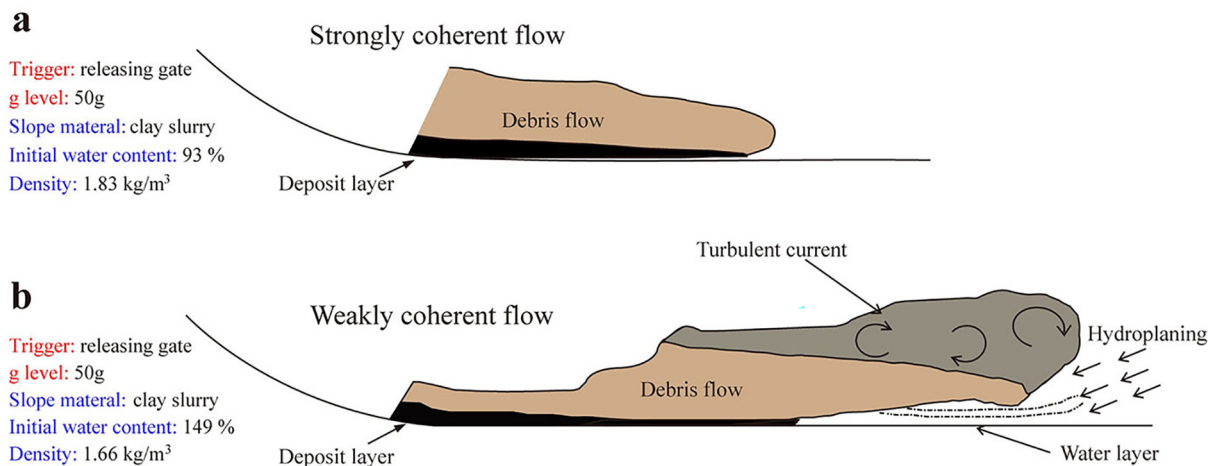


Fig. 24. Mobility of submarine debris flow through the releasing gate method: (a) strongly coherent flow; (b) weakly coherent flow (modified from Yin et al., 2019, reused with the permission of Taylor & Francis and Copyright Clearance Center).

process heater, is used in the centrifuge slope model. With the design of a novel atmospheric chamber equipped with two process heaters and compressed air, the swelling and shrinkage characteristics of clay slopes due to repetitive wet and dry seasons were tested at 60g (Take and Bolton, 2011). The accumulated downslope movements owing to dilation and softening of the clay slope resulted in slope failure over a long-term period. Seasonal deformation considered to be slope creep under fluctuating effective stress levels was also observed. By using a hernia lamp with wind circulation, wetting-drying cycles cause cumulated cracks and progressive failures (Chen et al., 2018). The construction of a cover layer was suggested to prevent such cracks. In addition, the seasonal effect on canal slopes was modelled at 50g by applying heat bulbs (Zhang et al., 2018a). The large deformation of the slope was only found in the first four cycles, which agreed with the depiction of the surface cracks and the strength in direct shear tests.

3.7.4. Other methods

To trigger an in-flight landslide, two specific methods using high-tech equipment are used. Chikatamarla et al. (2006) applied an electromagnet system to study the impact of rockfall on a cushion material. A guiding tube is applied to keep the boulder in the direction perpendicular to the cushion layer. A boulder made from microconcrete or steel was connected to a magnet block by electromagnetic force and released by switching off the electromagnet system. The other method is proposed to simulate submarine landslides triggered by gas hydrate dissociation (Zhang et al., 2015b). The process of gas hydrate dissociation in centrifuge tests was simplified by elevating the pore pressure at the base of the clayey slope with an air-water pressure control system. Pockmarks due to tensile failure and liquefaction were observed in gentler slopes and steeper slopes, respectively. In addition, recently, centrifuge tests with a combination of two major triggers for landslides have been carried out to further simulate the real circumstances (e.g., earthquake and rainfall in Xu et al., 2022; rainfall and water level fluctuation in Miao et al., 2022).

4. Centrifuge modelling of landslide mitigation

In terms of stabilisation methods, centrifuge modelling of landslide mitigation can include the application of nails, piles, geotextiles, vegetation and other methods.

4.1. Nails

In the soil nailed slope model, the nail materials, nail length and spacing of nails are the main factors affecting the slope stability. According to the different nail settings and triggering methods in centrifuge modelling, the effectiveness of the soil nail and the failure behaviour of the slope were investigated.

Under all conditions, including g-up, water level change, earthquake and external loading, nailed slopes with long nail lengths and short spacings showed less deformation and milder failures than unreinforced slopes (Shen et al., 1982; Deepa and Viswanadham, 2009; Wang et al., 2010a; Zhang et al., 2013). In the g-up test, deeper failure surfaces at higher g-levels occurred in the nail-reinforced slope. The occurrence of external failures and internal failures depended on the length and spacing of the nails (Zhang et al., 2001). When the nailed slope was subjected to a rising GWL, the delay and minimisation rather than prevention of local failures due to installation of soil nails were monitored at 30g (Zhou et al., 2006). A nail inclination of 10° could develop a larger nail axial force, which benefited slope stabilisation (Rotte and Viswanadham, 2013).

Concerning the performance of nails, nail pullout failure during failure and nail bending postfailure were observed (Tei et al., 1998). Based on the analysis of slope deformation, the maximum deflection locations of the nails were in the middle of the upper part and near the slope surface in the lower part (Zhang et al., 2013). In addition, a rock bolt, also considered to be a soil nailing method, was used in permafrost and dynamic centrifuge tests (Nakamoto et al., 2018). Plate bearing failures of small plates were the critical failure mechanism.

4.2. Piles

Stabilising piles or shafts are also applied as an effective mitigation method for landslides (Li et al., 2019b). The slope reinforcement mechanism is considered and explored through centrifuge modelling. The effects of the pile types, the spacing ratio of the piles and the location of the pile installation on slope stability were tested.

Generally, stabilising piles in slopes increase the stability level and decrease the deformation during g-up, earthquakes, rising GWLs and external loading (Takemura et al., 1994; Yoon and Ellis, 2009; Wang and Zhang, 2014; Di Laora and Fioravante, 2018). Regarding the spacing ratio, an effective pile spacing ratio

of 3.5–4 was confirmed in the slope under g-up and earthquake conditions (Al-Defae and Knappett, 2014; Lei and Wu, 2019). Although the wider spacing of piles was still able to contribute to slope stability during g-up (Yoon and Ellis, 2009), the failure mode may change from downslope failure to flow failure (Lei and Wu, 2019). Another critical aspect is the pile materials. By using elastic piles simulating idealised piles and microreinforced concrete piles representing the piles used on site in dynamic tests, reductions in permanent movements of 35% and 30%, respectively, were found at 50g. (Al-Defae and Knappett, 2014). Similar performances of aluminium piles and acrylic piles with lower bending stiffness were reported (Lei and Wu, 2019). Considering the different pile locations, spacing and types, four failure modes of piled slopes subjected to the g-up force and external loading were demonstrated (Zhang and Wang, 2017). Early centrifuge tests showed that the prevention of deformation by pile reinforcement was non-significant at the initial stage owing to seepage flows, while catastrophic landslides could be mitigated (Takemura et al., 1994).

Pile and slope behaviour were also analyzed by using strain gauges and image analysis in centrifuge tests. When dynamic loading was applied to pile-reinforced slopes, the maximum bending moments were located at the lower part of the pile (Yu et al., 2010). The measured bending moment decreased with a reduction in the spacing or slope inclination (Wang and Zhang, 2014). In addition, based on an analysis of an index called the diversity factor of displacement, the three processes, including the deformation localisation process, slip surface formation process and pile failure process, were illustrated (Zhang and Wang, 2016).

4.3. Geotextiles

The use of geotextiles is an attractive method for slope stabilisation owing to its shorter construction time. The functions and applications of geotextiles include reinforcement, separation, drainage, filtration and protection, which all favour landslide mitigation. Based on a specific type of geotextile with different vertical spacings, the effectiveness on slope stability was investigated with centrifuge modelling.

Regarding vertical spacing, a narrower spacing slope caused smaller deformation with fewer cracks under a change in the GWL at 50g (Hiro-oka et al., 2001) and sustained more significant

external loading from the strip footing at 40g (Sommers and Viswanadham, 2009). However, the failure mode, failure surfaces, settlements and location of maximum peak strain were independent of the spacing and tensile strength of the geotextiles in the g-up tests (Zornberg et al., 1998; Viswanadham and Mahajan, 2007). Regarding geotextile materials, the tensile strength of the geotextiles controlled the failure mode, including catastrophic failures and progressive failures (Viswanadham and Mahajan, 2007). Hybrid geosynthetics, which are a combination of permeable non-woven geotextiles and woven geogrids, can dissipate the PWP and retain slope stability in both seepage and rainfall conditions, as shown in Fig. 25 (Raisinghani and Viswanadham, 2011; Bhattacherjee and Viswanadham, 2019).

There are different observations regarding geotextile behaviours. Zornberg et al. (1997) found that the failure of the retrieved fabric was breakage instead of pullout in the g-up tests. In contrast, a possible pullout of the Pellon sheet was observed in the intense shaking test (Nova-Roessig and Sitar, 2006). These differences may occur due to the loading type and the location of the interaction between the geotextile and soil. Using digital image analysis, the maximum peak strain in the reinforcement layers occurred near the top of the slope, which was consistent with the largest overburden pressures (Sommers and Viswanadham, 2009). The distinct zones inside the geotextile reinforced slope subjected to g-up and drawdown could also be categorised from the image analysis (Luo et al., 2018).

In addition, the high-tech installation method for geotextiles during an in-flight was demonstrated with a minor disturbance in the slope model at 30g (Zimmie et al., 2005). Thusyanthan et al. (2007) selected a load cell with a pulley system to measure the tension of a geomembrane in an MSW slope during static and dynamic loading at 50g. Unlike the horizontal installation, a vertical geosynthetic reinforced soil slope experiencing a change in the GWL at 76.2g was performed to quantify the serviceability of the method (Jackson and Craig, 1998).

4.4. Vegetation

Vegetation is a cost-effective and environmentally friendly method and is widely used for slope protection. The influences from both the mechanical and hydrological aspects of vegetation

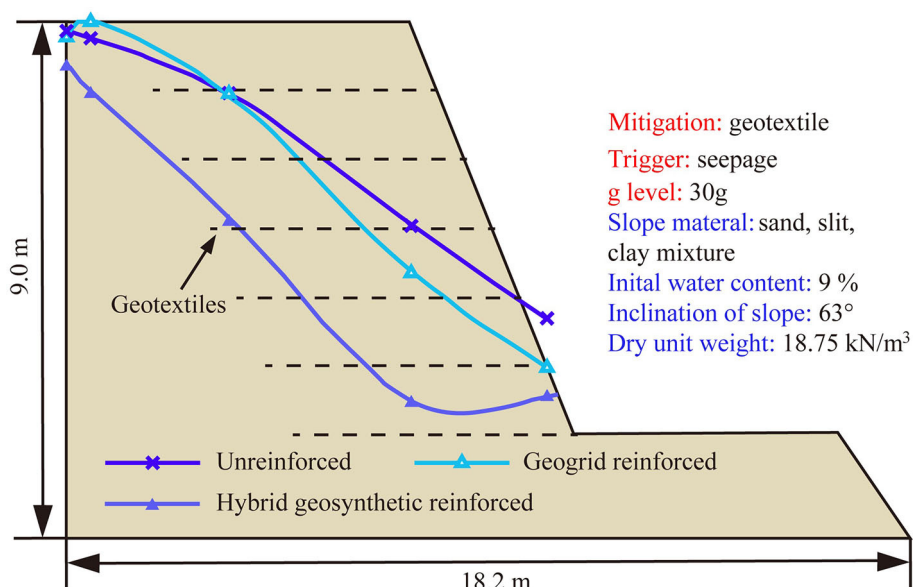


Fig. 25. Total head in geotextile-reinforced slopes (modified from Raisinghani and Viswanadham, 2011, reused with the permission of Elsevier and Copyright Clearance Center).

are distinct from those of other stabilisation methods. This method is a trend in the “green” direction for achieving sustainable development (Ng et al., 2016b). The centrifuge models of vegetation can be divided into the following three types: live roots, model roots and soil-fibre mixing (Ng et al., 2016a; Veenhof and Wu, 2018).

Due to the long-duration growth period before centrifuge spinning and the unknown distribution of live roots, centrifuge tests on live root-reinforced slopes are limited. Unlike progressive failures in nonvegetated areas during a rising water table at 15g, intact sliding occurred in slopes with willow vegetation (Sonnenberg et al., 2010). The interconnected network of roots inside the planted slope showed higher infiltration capacity during rainfall and increased slope stability. However, the vegetated slope might cause a larger failure volume when it fails (Askarinejad and Springman, 2015). By using fibre mixing, the slope failure time was delayed in the vegetated slope. This delay accompanied by slow slope movement enabled an early warning (Eab et al., 2015).

In the model roots, geometry is the key factor that affects slope stability. Branched roots, heart-shaped artificial roots and 3D root clusters showed better reinforcement performances in centrifuge slope models under water level changes, rainfall, and earthquakes, respectively (Sonnenberg et al., 2012; Leung et al., 2017; Liang et al., 2017). The tensile forces in the interaction between roots and soils were monitored as the primary reinforcement in the mechanical response (Sonnenberg et al., 2012). On the other hand, Ng et al. (2016b) focused on both the mechanical and hydrological effects of vegetation on a slope subjected to rainfall at 15g using a novel suction-controlled system, as shown in Fig. 26. Higher suction because of transpiration was observed and therefore contributed to lower infiltration. In addition, the root-reinforced method may be practical in planted slopes with modest heights to resist dynamic loading (Liang and Knappett, 2017).

4.5. Other methods

Water drainage attenuates erosion and decreases the destabilising force of hydrostatics and seepage, which is an important consideration in landslide mitigation. Apart from the surface drainage by geosynthetics or vegetation, Resnick and Znidarčić (1990) used horizontal porous bronze tubes to facilitate the subsurface drainage of an unstable slope subjected to a water level change at 100g. Singh et al. (2019) compared the effectiveness of steel drainage pipes, undrained steel pipes and silicone pipes in silty sand slopes. Better protection of steel drainage pipes in terms

of both drainage and stabilising function was found by comparison with the other two materials in seepage-induced landslides.

Aiming to mitigate the movement of flow-type landslides, the use of flexible barriers is a suitable method to dissipate the energy of landslides. Ng et al. (2017) used a model flexible barrier consisting of four steel strand cables to investigate the impact mechanisms of dry flow and viscous liquid by a releasing gate method at 22.4g, and the stored energies of the two materials were calculated as 73 kJ and 249 kJ, respectively. In a follow-up study, Song et al. (2018) tested five materials with different solid fractions and found that the barriers delivered flow loading to the upper cables of the barriers. A flexible barrier is an efficient tool for attenuating the impulse loads of entrained boulders in debris flows and debris avalanches (Song et al., 2019).

A combination of different stabilising techniques is favourable to advantage of the attributes of each method. An assembly of anchors and geosynthetics was used to evaluate the behaviour of slopes under a water level change at 50g (Rajabian et al., 2012). The restriction of lateral movements by passive anchored geosynthetics showed better slope stabilisation performance. Rajabian et al. (2013) further ascertained the effects of the stiffness and bond length of anchored geosynthetics on the stability of a lean clay slope. Zhao et al. (2014) tested the performance of a combined anchoring system consisting of prestressed model tiebacks and soil nails in mixed clayed sand and silty sand slopes. Huang et al. (2020) studied the seismic response of pile-anchor reinforced slopes at 50g. With most of the loading sustained by piles and outward movement restricted by anchors, the effectiveness of the combined structure during earthquakes was demonstrated. In addition, methods involving block reinforcement and large gabions were utilised in slopes under external and dynamic loading, respectively (Enomoto and Sasaki, 2018; Wang et al., 2018a).

5. Summary and recommendations for future research

The literature review presented existing research on centrifuge model tests to enhance our understanding of landslide behaviours and their mitigation methods. The basic deformation and failure mechanisms of landslides subjected to various triggers have been reviewed, together with the principles, scaling law and experimental considerations. The corresponding information about experimental techniques and test conditions for landslides were also summarised. We also presented centrifuge tests of landslides with various mitigation methods.

According to the principles and experimental considerations of centrifuge landslide models mentioned above, the success of a centrifuge landslide test is judged not only by its ability to demonstrate complex processes that match site observations but also by its ability to provide rigorous and reproducible results of qualitative behaviours and quantitative measurements. Therefore, careful preparation with an iterative process is necessary in centrifuge modelling of landslides, as shown in Fig. 27. The most effective criterion is the “modelling of models”. With the consideration of the research object of a landslide, the target of the modelling is first determined, which helps in selecting suitable scaling laws. The type and capacity of the centrifuge machine determine the selection of the g-level, the design of the test container, and the apparatus for triggering the landslide model. The test materials, the slope model construction method and the instrumentation for monitoring the deformation and failure process of the slope model are subsequently chosen. The basic parameters of the selected experimental materials and the accuracy of the equipment need to be checked carefully. After the model preparation, it is suggested that several preliminary tests be performed. If any abnormal behaviours of the slope model arise, the centrifuge landslide modelling

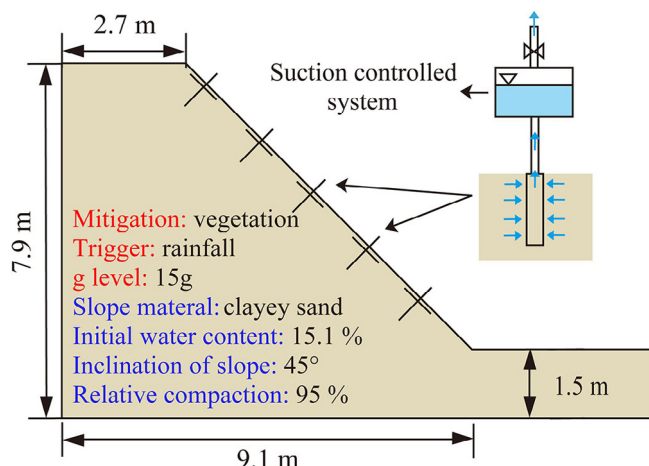


Fig. 26. Stability of the slope model reinforced by vegetation (modified from Ng et al., 2016b, reused with the permission of Springer Nature and Copyright Clearance Center).

design needs to be checked from the first step of the process. Notably, the practical limitations of each step during the tests need to be recorded and quantified. Finally, centrifuge landslide tests are carried out under the designed conditions.

The centrifuge modelling of landslides mentioned in the previous paragraph is an important part of the understanding, analysis and design of landslides under various conditions. Simulations of these conditions have been achieved by using the abovementioned methods. By simply increasing centrifugal acceleration without any other apparatus, rotational sliding failure in the soil slopes and toppling failure in the rock slopes were observed by using the unique triggering method. Rainfall simulations have been successfully applied by using spray nozzles. The change in pore water pressure during rainfall simulation determines the failure of soil slopes. The stability of earthquake-induced landslides has been studied using shaking tables with one or two shaking directions. Landslides subjected to water level changes and permafrost thawing were modeled with a water pump and warm air system, respectively. Various failure modes, including progressive failure, mudflow, flowslides, solifluction and detachment slides, were monitored under these two conditions. Landslide excavation was simulated by using a soil bag, pulley system and line-in-flight cut. In addition, a releasing gate, tilting table and heater have been used to achieve miscellaneous conditions and cause different slope failures. Table 8 summarizes the triggers previously used in centrifuge modelling applications for landslides and the resulting landslide behaviours.

At the laboratory scale, slopes reinforced with nails, piles, geotextiles, vegetation and other reinforcement approaches have been modelled successfully with centrifuge modelling. The results of such approaches include less deformation, less intense failure, fewer cracks, and a delay in the slope failure time. The detailed experimental monitoring demonstrates the change in the deformation and failure of slopes with these methods. The analysis of the influencing factor of each method, such as the reinforcement spacing, length, material properties, etc., highlights the effective design of methods for mitigating landslides. Table 9 summarizes the behaviors of the reinforced slopes and the performance of the reinforcing structures.

The deformation and failure mechanisms of a landslide are the physical, chemical or geological evolution processes that result in its failure. The mechanisms explain why, what, how, and when a landslide occurs. Based on the review of centrifuge landslide modelling with a focus on the mechanisms and landslide mitigation in this paper, some recommendations for centrifuge modelling for landslide and landslide mitigation are presented below.

(i) Landslide types with suitable model materials.

Based on the landslide-forming materials and modes of motion, a total of 32 landslide types were classified (Hung et al., 2014). The slope materials and model materials play a critical role in the initiation and propagation of landslides on site and in cen-

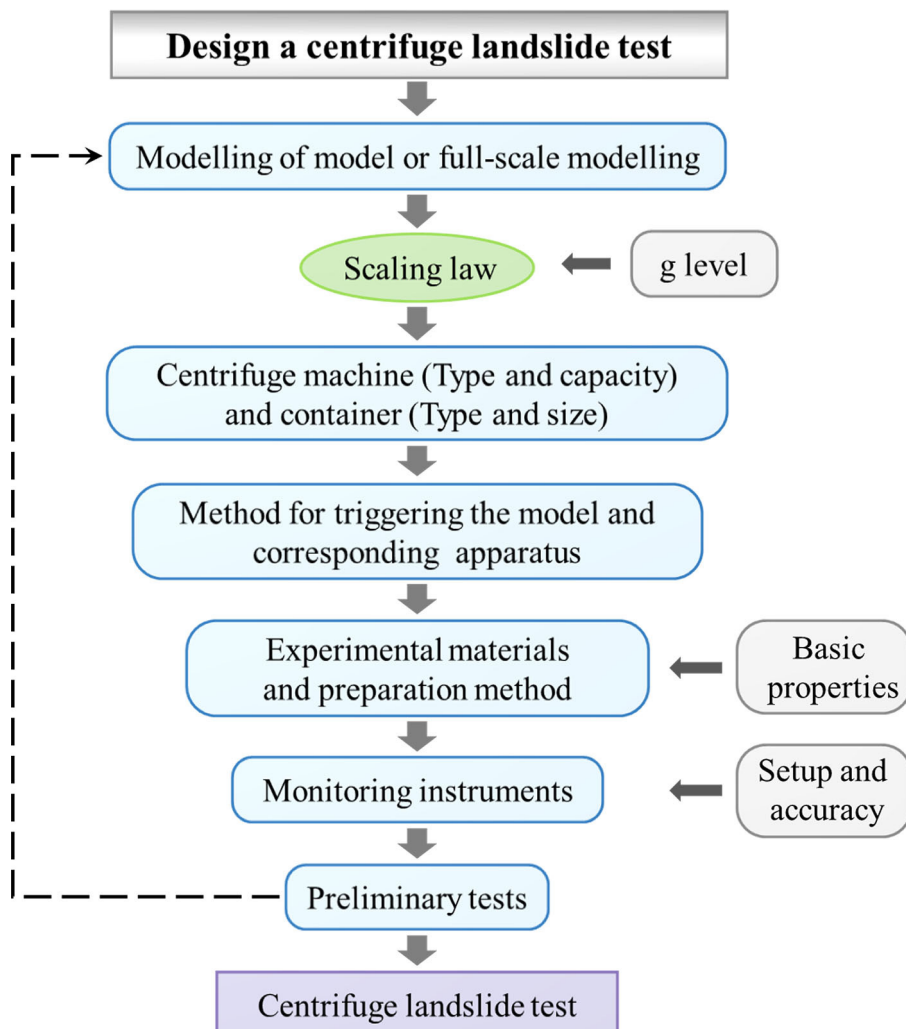


Fig. 27. Schematic for designing the centrifuge landslide test.

Table 8

Deformation and failure behaviour of landslide models under different triggers.

Trigger	Applications in centrifuge tests	Deformation and failure behaviour
Centrifugal acceleration	<ul style="list-style-type: none"> It is the easiest method for achieving deformation or failure of a landslide without any other apparatus The most widely used method for rock landslides The method is often used for validating analytical solutions 	<ul style="list-style-type: none"> Circular or noncircular rotational sliding surfaces are present in the soil slopes and the curvature surface is affected by the soil types, slope inclinations, degree of saturation and bedrock Block toppling, flexural toppling and block-flexural toppling are modelled in the rock centrifuge slope
Rainfall	<ul style="list-style-type: none"> Spray nozzles are mainly used to simulate slopes subjected to rainfall Most cases involve soil slopes 	<ul style="list-style-type: none"> The increase of negative PWP or the dissipation of positive PWP due to rainfall infiltration cause the failures of a soil slope
Earthquake	<ul style="list-style-type: none"> Shaking tables with one or two shaking directions are applied to simulate earthquakes Tests involve unsaturated and saturated soil slopes, rock slopes, and MSW slopes 	<ul style="list-style-type: none"> Amplifications of acceleration are monitored in the upper area of soil or rock-soil mixture slopes Deformation behaviour of unsaturated soil slope under seismic loading is affected by the shaking intensity, soil compaction, water content, and slope angle Multiple slip surfaces with broader shear bands are observed in saturated soil slopes, as well as void redistribution
Water level change	<ul style="list-style-type: none"> Ground water level and reservoir water level changes are mainly simulated by using a water pump system Soil slopes are the main slopes tested 	<ul style="list-style-type: none"> Progressive failures are recorded in a slope under reservoir water level fluctuations. The first fluctuation causes a larger deformation A wider slip surface and deformation area are present in a quick GWL change Static liquefaction of a loose slope is observed during the increase in the ground water flux
Warming permafrost	<ul style="list-style-type: none"> Warm air is used to model the process of thawing 	<ul style="list-style-type: none"> Soil slope failures including mudflow, flowslide, solifluction and detachment slide depend on the clay contents and stress conditions Frozen rock slopes are more at two temperatures
Excavation and external loading	<ul style="list-style-type: none"> Soil bag, pulley system and in-flight cut are applied to mimic an excavation process Surcharge and pneumatic pistons are modelled as external loads 	<ul style="list-style-type: none"> Local failure related to the arch action during excavation occurs in soil slopes The liquefaction of the slope model is monitored by applying an external load
Miscellaneous conditions	<ul style="list-style-type: none"> Various methods containing a releasing gate, tilting table, and heater are used 	<ul style="list-style-type: none"> Different failures, including rockfall, rock avalanche, and debris flow, are simulated in centrifuge modelling

Table 9

Deformation and failure behaviour of landslide models with different reinforcement methods.

Reinforcement method	Factors	Behaviour	Deformation and failure behaviour
Nails	Length, spacing of nails	<ul style="list-style-type: none"> Pullout failure and bending The middle of the upper part and near the slope surface in the lower part are the maximum deflection areas 	<ul style="list-style-type: none"> Long nail lengths and short spacings result in less deformation and mild failures
Piles	Material, diameter, spacing ratio	<ul style="list-style-type: none"> Maximum bending moments were located at the lower part of the pile 	<ul style="list-style-type: none"> An effective pile spacing ratio in the slope was 3.5–4 under g-up and earthquake conditions Downslope failure to flow failure occurred due to a wider spacing ratio
Geotextiles	Vertical spacing, tensile strength	<ul style="list-style-type: none"> Breakage and pull out are observed Maximum peak strain in the reinforcement layers occurred near the top of the slope 	<ul style="list-style-type: none"> A narrower spacing slope caused smaller deformation with fewer cracks and sustained more significant external loading The failure mode was independent of the spacing and tensile strength of the geotextiles A hybrid geosynthetic dissipated PWP and retained the slope stability
Vegetation	Material and geometry	–	<ul style="list-style-type: none"> The slope failure time was delayed in the vegetated slope Both mechanical and hydrological effects of vegetation were observed on a slope subjected to rainfall

trifuge models, respectively. As shown in Fig. 10, in terms of centrifuge model materials, the soil slopes were mainly modelled with sand, silt and clay. However, rock slopes can be simulated with various materials. Although existing research has studied the different types of landslides by using a variety of materials, further studies are needed to investigate the applicability of new materials to verify and demonstrate the hypothetical failure mechanisms in complex landslides.

(ii) Special design and equipment for landslide triggering and mitigation.

Observation of the full process of a landslide model subjected to a trigger is necessary for a centrifuge test. Triggering is achieved by using designed equipment during in-flight. Therefore, the devices

for triggering a landslide are of major significance in centrifuge modelling. In this review, g-up, rainfall, earthquakes, water table change, snowmelt, excavation, external loading and other methods are applied by using numerous high-tech apparatuses. Additionally, a special model reinforcement design uses 3D printer technology. Hence, further study of the development of devices and new technology with special designs is required to achieve more valuable simulations of landslides and their mitigation.

(iii) Measurement of landslide models.

The measurements of displacement and pressure are the prerequisites for analysing and understanding the deformation and failure behaviour of a landslide in centrifuge modelling. According to this review, the monitoring of surface displacement or slope

deformation has been updated from the traditional methods of markers, coloured layers, noodles, and films to advanced techniques (e.g., particle image velocimetry, digital image correlation, structure from motion, and optical fibres) (Take, 2015; Zhang et al., 2009, 2019b; Fang et al., 2021, 2022a). High soil suction can be reliably measured by new pore pressure transducers and tension transducers, which enables the observation of the change in negative PWP in a slope during rainfall. Tilt sensors and wave sensors are used to provide early warnings in rainfall-induced landslide models (Chen et al., 2019). Moreover, like multi-field monitoring in situ, a combination measurement system (e.g., the measurement of displacement, deformation, stress, pore water pressure in the surface, side and deep of a landslide model) is necessary for a landslide model test (Fang et al., 2022b). Therefore, further efforts to develop more accurate and functional measurement apparatuses are needed to provide more results and new insights into centrifuge slope models. Generally, measurement aspects in centrifuge modelling are suggested in two main directions: (a) more key parameters of landslides (e.g., directions of principal stresses, electrical resistivity, deep landslide displacements, acoustic emissions, etc.) through modified monitoring gauges or cutting-edge measurement techniques (b) data fusion technique (e.g., machine learning) for multi-source measurement data in centrifuge modelling.

(iv) Scaling laws.

Although conventional scaling laws of centrifuge modelling are well established and have been adopted for landslides and their mitigation, the scaling laws need to be modified or expanded for specific research purposes. At the grain scale, updated scaling laws were proposed to develop a static liquefaction mechanism for rainfall-induced landslides (Askarinejad et al., 2015). A partly reorganized, generalized scaling law was used to model mega earthquake-induced landslides with a scaling factor of up to 1000 (Zhou et al., 2019). In addition, hierarchical scaling laws using nondimensional variables were applied in flow-behaviour landslides, such as debris flows and dry flows (Bowman et al., 2010; Turnbull et al., 2015; Song et al., 2017). Further scaling law investigations are required for achieving better similarity between centrifuge models and prototype landslides. There are two primary improvements regarding scaling law in centrifuge modelling for landslides. To solve the difficulty of modelling large landslides owing to limited capacities of centrifuges and containers, developing new scaling laws that enable the utilization of current facilities is in demand. The other development is related to suitable scaling laws and validations for specific landslide modelling (e.g., debris flow) or specific mechanism (e.g., liquefaction).

(v) Full-scale centrifuge modelling for large landslides.

Full-scale centrifuge modelling is useful for directly guiding the construction and treatment of engineering communities. This modelling may require an advanced centrifuge machine with massive capacity, as well as careful preparation in terms of stress history in the prototype and external equipment for an identical conduction process in centrifuge modelling, especially for large landslide modelling. It is more important to fully understand the mechanisms of large landslides owing to their more serious destruction potential. Additionally, information from field monitoring is essential to support and compare with the results of full-scale slope tests, such as displacement, stress, strain, and water-level monitoring in the Huangtupo landslide, to provide basic data for evaluating a reservoir-induced landslide test (e.g., Tang et al., 2015, 2019; Li et al., 2019a; Li et al., 2021). Although many difficulties and limitations exist in full-scale slope mod-

elling for large landslides, many companies in Japan have built large centrifuge machines to assist in engineering construction. A centrifugal hypergravity and interdisciplinary experiment facility (CHIEF) with a maximum 1500g·t is under construction at Zhejiang University, China. Landslides are already considered to be among the most important topics in colossal projects. Therefore, further studies are needed to solve the critical problems in centrifuge modelling of large landslides. When more prototype large landslide behaviours are replicated and quantified at model scales, engineers may have more confidence in applying this technology.

(vi) Centrifuge modelling for landslide early warning.

Although many centrifuge models were developed and conducted for specific landslides, only a few models were applied for landslide forecasting and landslide early warning. For forecasting the time of failure of landslides, the integration of physical-based models and site investigations is promising. Four processes are crucial for this approach: first, the sufficient monitoring data and engineering geological conditions obtained from site investigations; secondly, the determination of analogous material and experimental process under centrifugal conditions; thirdly, the calculation of key parameters (e.g., displacement, velocity, tilt angle, and acoustic emission) that determines the slope failures through high accuracy measurement; finally, comparison and correction between the results from centrifuge models and field monitoring. Apart from developing these four procedures, research should focus on the development of methods for automatic model preparation. This is required for the elimination of operational error and the improvement of test reproducibility.

(vii) Centrifuge modelling for landslide from 2D to 3D.

Most centrifuge models for landslides are currently carried out in a 2D condition since 2D models have the advantage of simplifications. However, these simplifications may ignore valuable insights into the landslide mechanisms. 3D models have the major advantage that the shape and topography of landslide can be included in the resulting deformation and failure behaviours. Although 3D centrifuge modelling is still challenging work, a few attempts in 1g physical model offers the possibility of future centrifuge tests for landslides. Advanced techniques such as machining technology and 3D printers can provide complex topographic interferences according to the topographic map of landslides at sites. Likewise, there are also 3D measurement and monitoring techniques used such as 3D laser scanners and photogrammetry techniques have the potential to provide important ways to study 3D behaviour in model tests. Conducting 3D landslide models in centrifuge modelling based on these advanced techniques is expected to gradually bridge the gap between 2D models and landslides at sites.

Besides the above seven suggestions, a standardised and generalised summary of each experiment is necessary due to rapidly growing landslide research using centrifuge modelling. The variety of studies use different scales carried out, analysing tools used, sensors monitored, and landslide triggering configurations implemented, which is difficult to compare results with consistency. Based on the reviewed studies, a summary table should include the experimental aim, basic test information (e.g., test container, slope model, monitoring methods, and test conditions), and important results, which allows readers easily compare the experimental settings and results of different studies. An example of a standard protocol for a physical model test is shown in Table 10. Here, the brief and essential information in a test, instead of each detailed information, is suggested in the summarised table.

Table 10

Summarized protocol for a physical model test (an example of test data from Bhattacherjee and Viswanadham, 2019).

Test aim		Performance of reinforced slopes without specific prototype cases			
Basic	Triggers	Rainfall	Container	Rigid in beam centrifuge	
	g level	30		Length: 76 cm; width: 20 cm; height: 41cm	
	Landslide Classification ^{a)}	Sand slide		Compaction	
Slope model	Angle	63°	Reinforced model	Material ① PET + PVC; ② PP; ③ PET + PVC + PP	
	Material	sand–kaolin mix		Properties (PET + PVC) T_u : 0.93 and 2.02 kN/m ε_u : 18.9 and 24.2 %	
	Properties (sand)	G_s : 2.65; k : 1.5×10^{-4} m/s		Properties (PP) T_u : 0.25 kN/m ε_u : 9.89 %	
	Properties (kaolin)	LL: 41% PL: 14% k : 5×10^{-9} m/s		Properties (PET+PVC+PP) T_u : 1.01 and 2.08 kN/m ε_u : 18.3 and 22.8 %	
	Properties (mix)	γ_{dm} : 18.75 kN/m ³ ; k : 1.5×10^{-6} m/s			
Monitoring tool	Pore pressure transducers	Pore water pressure	Test condition	Test cases 7	
	Digital camera	Image analysis for displacements		Test variable Geosynthetic type and rainfall duration (9.4~22.0 days)	
Important results					
①	The peak strain in the nonwoven geotextile-reinforced slope was about 19% at the end of 15.6 days (prototype). However, lower peak strains of 8% and 3% at respective ultimate stages of 23.5 days and 18.8 days of rainfall in the two hybrid geosynthetics.				
②	In comparison to geogrid layers, hybrid geosynthetics reduced settlements and movements by 86% and 82% respectively. The pore-water pressures at the base in hybrid geosynthetic slopes were 40% and 26% less than that in the geogrid slopes and the geotextile-reinforced slopes, respectively.				

^{a)}: based on the updated Varnes classification system (Hung et al. 2014).

6. Conclusions

Centrifuge modelling has become an explorative simulation tool in the last ten years to understand the underlying mechanisms and evolutionary processes of landslides. In this context, we presented an overview of the deformation and failure characteristics of landslides subjected to various triggers through centrifuge modelling, including centrifugal acceleration, rainfall, earthquakes, water level changes, thawing permafrost, excavation, external loading and miscellaneous conditions. The applications and performances of the landslide models under the triggers have been discussed and linked to mechanisms. Meanwhile, the centrifuge modelling on landslide mitigation was also reviewed to study the usefulness of the reinforced methods of nails, piles, geotextiles, and vegetation.

Advances in operational equipment and monitoring methods during in-flight have sought to expedite and optimize the centrifuge landslide studies by the wide application of the equipment for the various triggers (e.g., rainfall and earthquake) and the extensive collections of multi-parameter measurements. Essential mechanisms of landslide (e.g., base liquefaction) and the effectiveness of the reinforced methods (e.g., vegetation) have been successfully conducted

and demonstrated with sophisticated experimental design through centrifuge modelling, which makes considerable progress in landslide science. In addition, many of the landslide behaviour monitored and observed from the centrifuge tests exceed the capability of existing analytical and numerical models.

Despite the significant advances in the research and development, challenges still exist in centrifuge modelling for landslides. These include issues such as the long-term behaviour of landslides through centrifuge modelling, the modelling of the control countermeasures for huge and long-runout landslides, the acquisition and data analyse of multi-field monitoring information, and the landslides prediction and early warning in centrifuge modelling. These challenges and difficulties provide opportunities for researchers and geological engineers in landslide reduction and mitigation.

Seven main aspects, including model material selections, sophisticated designs and instrumentation, high-tech and multi-field measurements, scaling laws, large landslides modelling, landslide early warning, and centrifuge modelling from 2D to 3D are recommended for future landslide research on centrifuge modelling. Besides, a suggested design process and a standardized

summary of a centrifuge test are necessary to effectively carry out centrifuge tests and increase the impact of experimental findings.

When a centrifugal landslide model test is planned, designed, conducted, and analyzed, it should be a valuable case study under a specific circumstance field investigation comparison, although a field study encompasses monitoring data of more complex and heterogeneous geomaterial characteristics. The controllable landslide initiation and boundary conditions, detailed and comprehensive measurements, concise and explicit experimental process, and reproducible slope behaviour in centrifuge modelling are more suitable for validating analytical and numerical methods. In addition, the current constitutive model and numerical modelling are not capable of reproducing the behaviour of the centrifugal landslide models mentioned in this review. Therefore, centrifuge modelling will play a more critical role and serve as an essential tool in landslide science.

With the continuous developments in centrifugal techniques for landslides, increasing investigations in this field will be launched. As Professor Phillips said, "Centrifuge model testing is a challenging and exciting experimental science", especially in landslide science mentioned by us.

CRediT authorship contribution statement

Kun Fang: Conceptualization, Methodology, Software, Formal analysis, Investigation, Visualization, Writing – original draft, Writing – review & editing. **Huiming Tang:** Resources, Funding acquisition, Writing – review & editing. **Changdong Li:** Writing – review & editing. **Xuexue Su:** Writing – review & editing. **Pengju An:** Writing – review & editing. **Sixuan Sun:** Writing – review & editing.

Declaration of Competing Interest

The authors declare that they have no known competing financial interests or personal relationships that could have appeared to influence the work reported in this paper.

Acknowledgements

This research is supported by National Major Scientific Instruments and Equipment Development Projects of China (Grant No.41827808), Major Program of the National Natural Science Foundation of China (Grant No. 42090055), the National Key Research and Development Program of China (Grant No.2017YFC1501305), and Development Program of Hubei Province of China (Grant No. 2020BCB079). The first author would like to gratitude to Assoc.Prof. Thirapong Pipatpongsa for his guidance. The authors sincerely thank Prof. Robert E. Criss, Prof. Jie Dou, and Dr. Jiawei Xu for their valuable suggestions and great support in this research. We thank Dr. Bingdong Ding, Dr. Bocheng Zhang, Dr. Minghao Miao, Dr. Chunyan Tang, Dr. Wenmin Yao, Dr. Yibing Ning, Dr. Chao Huang, Dr. Nan Li for comments that greatly improved the manuscript. We would also like to show our gratitude to Prof. Sarah M. Springman, Dr. Wilmer Ferney Morales Peñuela, Assoc.Prof. Kyohei Ueda, Prof. Kazuya Itoh, Prof. Akihiko Wakai, and Ms. Ayako Namigishi for sharing and provided documents with us in this research. We thank the editors and the three anonymous reviewers in Geoscience Frontiers for their insights.

References

- Acosta, E.A., Tibana, S., de Almeida, M.d.S.S., Saboya Jr, F., 2017. Centrifuge modeling of hydroplaning in submarine slopes. *Ocean Eng.* 129, 451–458. <https://doi.org/10.1016/j.oceaneng.2016.10.047>.
- Adhikary, D., Dyskin, A., 2007. Modelling of progressive and instantaneous failures of foliated rock slopes. *Rock Mech. Rock Eng.* 40 (4), 349–362. <https://doi.org/10.1007/s00603-006-0085-8>.
- Adhikary, D., Dyskin, A., Jewell, R., Stewart, D., 1997. A study of the mechanism of flexural toppling failure of rock slopes. *Rock Mech. Rock Eng.* 30 (2), 75–93. <https://doi.org/10.1007/BF01020126>.
- Al-Defae, A., Knappett, J., 2014. Centrifuge modeling of the seismic performance of pile-reinforced slopes. *J. Geotech. Geoenviron.* 140 (6), 04014014. [https://doi.org/10.1061/\(ASCE\)GT.1943-5606.0001105](https://doi.org/10.1061/(ASCE)GT.1943-5606.0001105).
- Askarinejad, A., Springman, S.M. 2015. Centrifuge modelling of the effects of vegetation on the response of a silty sand slope subjected to rainfall, Computer Methods and Recent Advances in Geomechanics: Proceedings of the 14th International Conference of International Association for Computer Methods and Recent Advances in Geomechanics, 2014 (IACMAG 2014). Taylor & Francis Books Ltd. 1339–1344.
- Askarinejad, A., Beck, A., Springman, S.M., 2015. Scaling law of static liquefaction mechanism in geocentrifuge and corresponding hydromechanical characterization of an unsaturated silty sand having a viscous pore fluid. *Can. Geotech. J.* 52 (6), 708–720. <https://doi.org/10.1139/cgj-2014-0237>.
- Avgerinos, P., Schofield, A. 1969. Drawdown failure of centrifuge models. *Proc. of 7th ICSMFE.* 2, 497–506.
- Azevedo, R., Ko, H., 1988. In-flight centrifuge excavation tests in sand, *Int. Paris, Balkema*, pp. 119–124. Conf. Centrifuge88.
- Beasley, D.H. 1973. Centrifugal modelling of soft clay strata subject to embankment loading. *University of Cambridge*.
- Beddoe, R.A., Take, W.A., 2015. Influence of slope inclination on the triggering and distal reach of hydraulically-induced flow slides. *Eng. Geol.* 187, 170–182. <https://doi.org/10.1016/j.enggeo.2015.01.006>.
- Bhattacharjee, D., Viswanadham, B., 2019. Centrifuge Model Studies on Performance of Hybrid Geosynthetic-Reinforced Slopes with Poorly Draining Soil Subjected to Rainfall. *J. Geotech. Geoenviron.* 145 (12), 04019108. [https://doi.org/10.1061/\(ASCE\)GT.1943-5606.0002168](https://doi.org/10.1061/(ASCE)GT.1943-5606.0002168).
- Bowman, E.T., Laue, J., Imre, B., Springman, S.M., 2010. Experimental modelling of debris flow behaviour using a geotechnical centrifuge. *Can. Geotech. J.* 47 (7), 742–762. <https://doi.org/10.1139/T09-141>.
- Bowman, E.T., Take, W.A., Rait, K., Hann, C., 2012. Physical models of rock avalanche spreading behaviour with dynamic fragmentation. *Can. Geotech. J.* 49 (4), 460–476. <https://doi.org/10.1139/12012-007>.
- Bowman, E.T., Take, W.A., 2015. The runout of chalk cliff collapses in England and France—case studies and physical model experiments. *Landslides* 12 (2), 225–239. <https://doi.org/10.1007/s10346-014-0472-2>.
- Brennan, A., Madabhushi, S., 2009. Amplification of seismic accelerations at slope crests. *Can. Geotech. J.* 46 (5), 585–594. <https://doi.org/10.1139/T09-006>.
- Bryant, S., Take, W.A., Bowman, E., Millen, M., 2015. Physical and numerical modelling of dry granular flows under Coriolis conditions. *Géotechnique* 65 (3), 188–200. <https://doi.org/10.1680/geot.13.P.208>.
- Cabrera, M.A., Wu, W., 2017. Experimental modelling of free-surface dry granular flows under a centrifugal acceleration field. *Granul. Matter* 19 (4), 78. <https://doi.org/10.1007/s10035-017-0764-z>.
- Chen, Z., Gong, W., Ma, G., Wang, J., He, L., Xing, Y., Xing, J., 2015. Comparisons between centrifuge and numerical modeling results for slope toppling failure. *Sci. China Technol. Sci.* 58 (9), 1497–1508. <https://doi.org/10.1007/s11431-015-5889-x>.
- Chen, X., Huang, J., 2011. Stability analysis of bank slope under conditions of reservoir impounding and rapid drawdown. *J. Rock Mech. Geotech. Eng.* 3, 429–437. <https://doi.org/10.3724/SJ.1235.2011.00429>.
- Chen, Y., Irfan, M., Uchimura, T., Wu, Y., Yu, F., 2019. Development of elastic wave velocity threshold for rainfall-induced landslides prediction and early warning. *Landslides* 16 (5), 955–968. <https://doi.org/10.1007/s10346-019-01138-2>.
- Chen, Y.M., Li, J.C., Yang, C.B., Zhu, B., Zhan, L.T., 2017. Centrifuge modeling of municipal solid waste landfill failures induced by rising water levels. *Can. Geotech. J.* 54 (12), 1739–1751. <https://doi.org/10.1139/cgj-2017-0046>.
- Chen, T.-L., Zhou, C., Wang, G.-L., Liu, E.-L., Dai, F., 2018. Centrifuge model test on unsaturated expansive soil slopes with cyclic wetting-drying and inundation at the slope toe. *International Journal of Civil Engineering* 16, 1341–1360. <https://doi.org/10.1007/s40999-017-0228-1>.
- Cheng, Y., Cheng, Z., Zhang, Y., 2011. Centrifugal model tests on expansive soil slope under rainfall. *Chinese J. Geotech. Eng.* 33 (1), 409–414.
- Chikatamarla, R., Laue, J., Springman, S.M., 2006. Centrifuge scaling laws for guided free fall events including rockfalls. *Int. J. Phys. Model. Geo.* 6 (2), 15–26. <https://doi.org/10.1680/ijpmg.2006.060202>.
- Collins, B.D., Znidarcic, D., 2004. Stability analyses of rainfall induced landslides. *J. Geotech. Geoenviron.* 130 (4), 362–372. [https://doi.org/10.1061/\(ASCE\)1090-0241\(2004\)130:4\(362\)](https://doi.org/10.1061/(ASCE)1090-0241(2004)130:4(362)).
- Cruden, D.M., Varnes, D.J. 1996. Landslides: investigation and mitigation. Chapter 3-Landslide types and processes. Transportation research board special report. (247).
- Davies, M.C., Hamza, O., Harris, C., 2001. The effect of rise in mean annual temperature on the stability of rock slopes containing ice-filled discontinuities. *Permafrost Periglac.* 12 (1), 137–144. <https://doi.org/10.1002/ppp.378>.
- Deepa, V., Viswanadham, B., 2009. Centrifuge model tests on soil-nailed slopes subjected to seepage. *Proceedings of the Institution of Civil Engineers-Ground Improvement* 162 (3), 133–144. <https://doi.org/10.1680/grim.2009.162.3.133>.
- Di Laora, R., Fioravante, V., 2018. A method for designing the longitudinal spacing of slope-stabilizing shafts. *Acta Geotechnica* 13 (5), 1141–1153. <https://doi.org/10.1007/s11440-017-0617-2>.
- Duncan, J.M., Wright, S.G., Brandon, T.L., 2014. *Soil strength and slope stability*. John Wiley & Sons.

- Eab, K.H., Likitlersuang, S., Takahashi, A., 2015. Laboratory and modelling investigation of root-reinforced system for slope stabilisation. *Soils Found.* 55 (5), 1270–1281. <https://doi.org/10.1016/j.sandf.2015.09.025>.
- Enomoto, T., Sasaki, T., 2015. Several factors affecting seismic behaviour of embankments in dynamic centrifuge model tests. *Soils Found.* 55 (4), 813–828. <https://doi.org/10.1016/j.sandf.2015.06.013>.
- Enomoto, T., Sasaki, T., 2018. Seismic behaviour of reinforced embankments in dynamic centrifuge model tests. *Soils Found.* 58 (1), 212–227. <https://doi.org/10.1016/j.sandf.2017.12.005>.
- Fan, Z., Kulatilake, P., Peng, J., Che, W., Li, Y., Meng, Z., 2016. In-flight excavation of a loess slope in a centrifuge model test. *Geotech. Eng.* 34 (5), 1577–1591. <https://doi.org/10.1007/s10706-016-0067-x>.
- Fan, L., Zhang, G., Li, B., Tang, H., 2017. Deformation and failure of the Xiaochatou Landslide under rapid drawdown of the reservoir water level based on centrifuge tests. *B. Eng. Geol. Environ.* 76 (3), 891–900. <https://doi.org/10.1007/s10064-016-0895-1>.
- Fang, K., 2019. Progression and onset of undercut slope failure observed by surface velocity in physical models subjected to arch action. Kyoto University.
- Fang, K., An, P., Tang, H., Tu, J., Jia, S., Miao, M., Dong, A., 2021. Application of a multi-smartphone measurement system in slope model tests. *Engineering Geology* 106424. <https://doi.org/10.1016/j.enggeo.2021.106424>.
- Fang, K., Miao, M., Tang, H., Dong, A., Jia, S., An, P., Zhang, B., Tu, J., 2022a. Model test on deformation and failure behaviour of arching-type slope under excavation condition. *Engineering Geology* 106628.
- Fang, K., Miao, M., Tang, H., Jia, S., Dong, A., An, P., Zhang, B., 2022b. Insights into the deformation and failure characteristic of a slope due to excavation through multi-field monitoring: a model test. *Acta Geotechnica*.
- Fredlund, D.G., Rahardjo, H., Fredlund, M.D., 2012. *Unsaturated Soil Mechanics in Engineering Practice*. John Wiley & Sons.
- Goldstein, M., Berman, M., Goose, B., Timofeyeva, T., Turovskaya, A. 1966. Stability investigation of fissured rock slopes. 1st ISRM Congress.
- Goodings, D., Schofield, A., 1985. A centrifugal model study of slope instability in Ottawa area Champlain Sea clay. *Can. Geotech. J.* 22 (1), 102–109. <https://doi.org/10.1139/t85-010>.
- Gue, C., Soga, K., Bolton, M., Thusyanthan, N., 2010. Centrifuge modelling of submarine landslide flows. *Stress* 32 (2), 8. <https://doi.org/10.1201/b10554-183>.
- Harris, C., Rea, B., Davies, M., 2001. Scaled physical modelling of mass movement processes on thawing slopes. *Permafrost Periglac.* 12 (1), 125–135. <https://doi.org/10.1002/ppg.373>.
- Harris, C., Davies, M.C., Rea, B.R., 2003. Gelification: viscous flow or plastic creep? *Earth Surface Processes and Landforms: The Journal of the British Geomorphological Research Group* 28 (12), 1289–1301. <https://doi.org/10.1002/esp.543>.
- Harris, C., Smith, J.S., Davies, M.C., Rea, B., 2008. An investigation of periglacial slope stability in relation to soil properties based on physical modelling in the geotechnical centrifuge. *Geomorphology* 93 (3–4), 437–459. <https://doi.org/10.1016/j.geomorph.2007.03.009>.
- Highland, L., Bobrowsky, P.T., 2008. *The landslide handbook: a guide to understanding landslides*. US Geological Survey Reston.
- Higo, Y., Lee, C.-W., Doi, T., Kinugawa, T., Kimura, M., Kimoto, S., Oka, F., 2015. Study of dynamic stability of unsaturated embankments with different water contents by centrifugal model tests. *Soils Found.* 55 (1), 112–126. <https://doi.org/10.1016/j.sandf.2014.12.009>.
- Hiro-oka, A., Kobayashi, M., Nagase, H., Shimizu, K. 2001. Performance of geotextile reinforced slopes subjected to seepage flow. *Landmarks in earth reinforcement*. Edited by H. Ochiai, J. Otani, N. Yasufuku, and K. Omine. Swets & Zeitlinger. 207–212.
- Hu, Y., Zhang, G., Zhang, J.-M., Lee, C., 2010. Centrifuge modeling of geotextile-reinforced cohesive slopes. *Geotextiles and Geomembranes* 28, 12–22. <https://doi.org/10.1016/j.geotexmem.2009.09.001>.
- Huang, Y., Xu, X., Liu, J., Mao, W., 2020. Centrifuge modeling of seismic response and failure mode of a slope reinforced by a pile-anchor structure. *Soil Dyn. Earthq. Eng.* 131, 106037. <https://doi.org/10.1016/j.soildyn.2020.106037>.
- Huang, Y., Zhang, B., 2020. Review on key issues in centrifuge modeling of flow-structure interaction. *Eur. J. Environ. Civ.*, 1–17 <https://doi.org/10.1080/19648189.2020.1762751>.
- Hung, W.Y., Tran, M.C., Yeh, F.H., Lu, C.W., Ge, L., 2020. Centrifuge modeling of failure behaviors of sandy slope caused by gravity, rainfall, and base shaking. *Eng. Geol.* 105609. <https://doi.org/10.1016/j.enggeo.2020.105609>.
- Hungr, O., Leroueil, S., Picarelli, L., 2014. The Varnes classification of landslide types, an update. *Landslides* 11 (2), 167–194. <https://doi.org/10.1007/s10346-013-0436-y>.
- Idlinger, G., Wu, W., 2019. Failure of Unsaturated Soil Slopes Initiated by Self-weight Loading. *Recent Advances in Geotechnical Research*. Springer, 91–103. https://doi.org/10.1007/978-3-319-89671-7_8.
- Itoh, K., Timpone, S., Toyosawa, Y., Tamrakar, S., Suemasa, N. 2009a. Physical modeling of slope failure during slope cutting work, Proceedings of the 17th International Conference on Soil Mechanics and Geotechnical Engineering, Alexandria. 522–525.
- Itoh, K., Toyosawa, Y., Kusakabe, O., 2009b. Centrifugal modelling of rockfall events. *Int. J. Phys. Model. Geo.* 9 (2), 01–22.
- Ivanov, V., Longoni, L., Ferrario, M., Brunero, M., Arosio, D., Papini, M., 2021. Applicability of an interferometric optical fibre sensor for shallow landslide monitoring–Experimental tests. *Engineering Geology* 288, 106128. <https://doi.org/10.1016/j.enggeo.2021.106128>.
- Jackson, A.M.R., Craig, W.H., 1998. Modelling vertical geosynthetic reinforcement of soil slopes. *Centrifuge* 98, 753–759.
- Khosravi, M., Takemura, J., Pipatpongsoa, T. 2013. Centrifugal modeling of undercut slopes subjected to pseudo-static loading, The 10th International Conference on Urban Earthquake Engineering, 523–532.
- Khosravi, M.H., Takemura, J., Pipatpongsoa, T., Amini, M., 2016. In-Flight Excavation of Slopes with Potential Failure Planes. *J. Geotech. Geoenviron.* 142 (5). [https://doi.org/10.1061/\(ASCE\)GT.1943-5606.0001439](https://doi.org/10.1061/(ASCE)GT.1943-5606.0001439).
- Kim, D.-S., Kim, N.-R., Choo, Y.-W., 2009. Physical modeling of geotechnical systems using centrifuge. *Proceedings of the Korean Geotechnical Society Conference*. Korean Geotechnical Society, 194–205.
- Kimura, T., 1991. *Failure of fills due to rain fall*. Centrifuge. Balkema, 509–516.
- Kulasingam, R., Malwick, E.J., Boulanger, R.W., Kutter, B.L., 2004. Strength loss and localization at silt interlayers in slopes of liquefied sand. *J. Geotech. Geoenviron.* 130 (11), 1192–1202. [https://doi.org/10.1061/\(ASCE\)1090-0241\(2004\)130:11\(1192\)](https://doi.org/10.1061/(ASCE)1090-0241(2004)130:11(1192)).
- Kutter, B.L., 2020. *Model Tests and Numerical Simulations of Liquefaction and Lateral Spreading*. Springer Nature.
- Kutter, B.L., James, R., 1989. Dynamic centrifuge model tests on clay embankments. *Geotechnique* 39 (1), 91–106. <https://doi.org/10.1680/geot.1989.39.1.91>.
- Lee, Y., Cheuk, C., Bolton, M., 2008. Instability caused by a seepage impediment in layered fill slopes. *Can. Geotech. J.* 45 (10), 1410–1425. <https://doi.org/10.1139/T08-067>.
- Lee, L.M., Kassim, A., Gofar, N., 2011. Performances of two instrumented laboratory models for the study of rainfall infiltration into unsaturated soils. *Engineering Geology* 117, 78–89. <https://doi.org/10.1016/j.enggeo.2010.10.007>.
- Lei, G., Wu, W., 2019. Centrifuge study on the effect of pile bending stiffness on the slope stabilised by piles. *Int. J. Phys. Model. Geo.*, 1–12 <https://doi.org/10.1680/jphmg.18.00087>.
- Leroueil, S., 2001. Natural slopes and cuts: movement and failure mechanisms. *Geotechnique* 51 (3), 197–243. <https://doi.org/10.1680/geot.2001.51.3.197>.
- Leung, A.K., Kamchoom, V., Ng, C.W.W., 2017. Influences of root-induced soil suction and root geometry on slope stability: a centrifuge study. *Can. Geotech. J.* 54 (3), 291–303. <https://doi.org/10.1139/cgj-2015-0263>.
- Li, B., Feng, Z., Wang, G., Wang, W., 2016. Processes and behaviors of block topple avalanches resulting from carbonate slope failures due to underground mining. *Environ. Earth Sci.* 75 (8), 694. <https://doi.org/10.1007/s12665-016-5529-1>.
- Li, C., Fu, Z., Wang, Y., Tang, H., Yan, J., Gong, W., Yao, W., Criss, R.E., 2019a. Susceptibility of reservoir-induced landslides and strategies for increasing the slope stability in the Three Gorges Reservoir Area: Zigui Basin as an example. *Eng. Geol.* 261, 105279.
- Li, L.Q., Ju, N.P., Guo, Y.X., 2017. Effectiveness of Fiber Bragg Grating monitoring in the centrifugal model test of soil slope under rainfall conditions. *J. Mt. Sci.* 14 (5), 936–947. <https://doi.org/10.1007/s11629-016-4163-4>.
- Li, S., Knappett, J., Feng, X., 2015a. Investigation of slope stability influenced by change of reservoir water level in three Gorges of China. *Physical and Numerical Simulation of Geotechnical Engineering* 18, 49.
- Li, X., Tang, H., Xiong, C., Wartman, J., Yin, Y., 2015b. *Dynamic centrifuge modelling tests for toppling rock slopes*, *Engineering Geology for Society and Territory-Volume 2*. Springer, 769–774.
- Li, S., Xu, Q., Tang, M., Li, H., Yang, H., Wei, Y., 2020. Centrifuge Modeling and the Analysis of Ancient Landslides Subjected to Reservoir Water Level Fluctuation. *Sustainability* 12 (5), 2092. <https://doi.org/10.3390/su12052092>.
- Li, C., Yan, J., Wu, J., Lei, G., Wang, L., Zhang, Y., 2019b. Determination of the embedded length of stabilizing piles in colluvial landslides with upper hard and lower weak bedrock based on the deformation control principle. *B. Eng. Geol. Environ.* 78 (2), 1189–1208.
- Li, C., Criss, R.E., Fu, Z., Long, J., Tan, Q., 2021. Evolution characteristics and displacement forecasting model of landslides with stair-step sliding surface along the Xiangxi River, three Gorges Reservoir region, China. *Eng. Geol.* 105961. <https://doi.org/10.1016/j.enggeo.2020.105961>.
- Li, M., Zhang, G., Zhang, J.M., Lee, C., 2011. Centrifuge model tests on a cohesive soil slope under excavation conditions. *Soils Found.* 51 (5), 801–812. <https://doi.org/10.3208/sandf.51.801>.
- Liang, T., Knappett, J., 2017. Centrifuge modelling of the influence of slope height on the seismic performance of rooted slopes. *Geotechnique* 67 (10), 855–869. <https://doi.org/10.1680/jgeot.16.P.072>.
- Liang, T., Knappett, J., Bengough, A., Ke, Y., 2017. Small-scale modelling of plant root systems using 3D printing, with applications to investigate the role of vegetation on earthquake-induced landslides. *Landslides* 14 (5), 1747–1765. <https://doi.org/10.1007/s10346-017-0802-2>.
- Ling, H., Ling, H.I., 2012. Centrifuge model simulations of rainfall-induced slope instability. *J. Geotech. Geoenviron.* 138 (9), 1151–1157. [https://doi.org/10.1061/\(ASCE\)GT.1943-5606.0000679](https://doi.org/10.1061/(ASCE)GT.1943-5606.0000679).
- Ling, H.I., Wu, M.-H., Leshchinsky, D., Leshchinsky, B., 2009. Centrifuge modeling of slope instability. *J. Geotech. Geoenviron.* 135 (6), 758–767. [https://doi.org/10.1061/\(ASCE\)GT.1943-5606.0000024](https://doi.org/10.1061/(ASCE)GT.1943-5606.0000024).
- López, C.L., Garzón, L.X., Campagnoli, S.X., 2021. Geotechnical centrifuge applications in the teaching of applied soil mechanics. *Revista Educación en Ingeniería* 16, 10–15. <https://doi.org/10.26507/rei.v16n32.1188>.

- Lü, X., Xue, D., Chen, Q., Zhai, X., Huang, M., 2019. Centrifuge model test and limit equilibrium analysis of the stability of municipal solid waste slopes. *B. Eng. Geol. Environ.* 78 (4), 3011–3021. <https://doi.org/10.1007/s10064-018-1308-4>.
- Lucas, D., Herzog, R., Iten, M., Buschor, H., Kieper, A., Askarinejad, A., Springman, S. M., 2019. Modelling of landslides in a screen slope induced by groundwater and rainfall. *Int. J. Phys. Model. Geo.*, 1–21 <https://doi.org/10.1680/jphmg.18.00106>.
- Luo, F., Zhang, G., 2016. Progressive failure behavior of cohesive soil slopes under water drawdown conditions. *Environ. Earth Sci.* 75 (11), 973. <https://doi.org/10.1007/s12665-016-5802-3>.
- Luo, F., Zhang, G., Liu, Y., Ma, C., 2018. Centrifuge modeling of the geotextile reinforced slope subject to drawdown. *Geotext. Geomembranes* 46 (1), 11–21. <https://doi.org/10.1016/j.geotexmem.2017.09.001>.
- Lyndon, A., Schofield, A., 1970. Centrifugal model test of a short-term failure in London clay. *Geotechnique* 20 (4), 440–442. <https://doi.org/10.1680/geot.1970.20.4.440>.
- Lyndon, A., Schofield, A., 1978. Centrifugal model tests of the Lodalen landslide. *Can. Geotech. J.* 15 (1), 1–13. <https://doi.org/10.1139/t78-001>.
- Maghsoudloo, A., Askarinejad, A., de Jager, R.R., Molenkamp, F., Hicks, M.A., 2021. Large-scale physical modelling of static liquefaction in gentle submarine slopes. *Landslides* 18, 3315–3335. <https://doi.org/10.1007/s10346-021-01705-6>.
- Malwick, E.J., Kutter, B.L., Boulanger, R.W., 2008. Postshaking shear strain localization in a centrifuge model of a saturated sand slope. *J. Geotech. Geoenviron.* 134 (2), 164–174. [https://doi.org/10.1061/\(ASCE\)1090-0241\(2008\)134:2\(164\)](https://doi.org/10.1061/(ASCE)1090-0241(2008)134:2(164)).
- Matsuoa, O., Saito, Y., Sasaki, T., Kondoh, K., Sato, T., 2002. Earthquake-induced flow slides of fills and infinite slopes. *Soils Found.* 42 (1), 89–104. <https://doi.org/10.3208/sandf.42.89>.
- Miao, F., Wu, Y., Li, L., Tang, H., Li, Y., 2018. Centrifuge model test on the retrogressive landslide subjected to reservoir water level fluctuation. *Eng. Geol.* 245, 169–179. <https://doi.org/10.1016/j.enggeo.2018.08.016>.
- Miao, F., Wu, Y., Török, Á., Li, L., Xue, Y., 2022. Centrifugal model test on a riverine landslide in the three gorges reservoir induced by rainfall and water level fluctuation. *Geoscience Frontiers* 101378. <https://doi.org/10.1016/j.gsf.2022.101378>.
- Milne, F., Brown, M., Knappett, J., Davies, M., 2012. Centrifuge modelling of hillslope debris flow initiation. *Catena* 92, 162–171. <https://doi.org/10.1016/j.catena.2011.12.001>.
- Mitchell, R.J., 1970. On the yielding and mechanical strength of Leda clays. *Canadian Geotechnical Journal* 7, 297–312. <https://doi.org/10.1139/t70-036>.
- Morales Peñuela, W.F. 2013. River dyke failure modeling under transient water conditions. ETH Zurich.
- Moriwaki, H., Inokuchi, T., Hattanji, T., Sassa, K., Ochiai, H., Wang, G., 2004. A fluidized landslide on a natural slope by artificial rainfallFailure processes in a full-scale landslide experiment using a rainfall simulator. *Landslides* 1 (4), 277–288. <https://doi.org/10.1007/s10346-004-0034-0>.
- Nakamoto, S., Iwasa, N., Takemura, J., 2017. Effects of nails and facing plates on seismic slope response and failure. *Géotechnique Letters* 7, 136–145. <https://doi.org/10.1680/gjele.16.00179>.
- Nakamoto, S., Iwasa, N., Takemura, J., 2018. Centrifuge modelling of rock bolts with facing plates. *Int. J. Phys. Model. Geo.* 18 (1), 21–32. <https://doi.org/10.1680/jphmg.16.00006>.
- Ng, C.W.W., 2014. The state-of-the-art centrifuge modelling of geotechnical problems at HKUST. *J. Zhejiang Univ. Sci. A* 15, 1–21. <https://doi.org/10.1631/jzus.A1300217>.
- Ng, C.W.W., Li, X.-S., Van Laak, P.A., Hou, D.Y., 2004. Centrifuge modeling of loose fill embankment subjected to uni-axial and bi-axial earthquakes. *Soil Dyn. Earthq. Eng.* 24 (4), 305–318. <https://doi.org/10.1016/j.soildyn.2003.12.002>.
- Ng, C.W.W., Leung, A.K., Yu, R., Kamchoom, V., 2016a. Hydrological effects of live poles on transient seepage in an unsaturated soil slope: centrifuge and numerical study. *Geotech. Geoenviron.* 143 (3), 1–9.
- Ng, C.W.W., Kamchoom, V., Leung, A.K., 2016b. Centrifuge modelling of the effects of root geometry on transpiration-induced suction and stability of vegetated slopes. *Landslides* 13 (5), 925–938.
- Ng, C.W.W., Song, D., Choi, C.E., Liu, L., Kwan, J.S.H., Koo, R., Pun, W.K., 2017. Impact mechanisms of granular and viscous flows on rigid and flexible barriers. *Can. Geotech. J.* 54 (2), 188–206. <https://doi.org/10.1139/cgj-2016-0128>.
- Nova-Roessig, L., Sitar, N., 2006. Centrifuge model studies of the seismic response of reinforced soil slopes. *J. Geotech. Geoenviron.* 132 (3), 388–400. [https://doi.org/10.1061/\(ASCE\)1090-0241\(2006\)132:3\(388\)](https://doi.org/10.1061/(ASCE)1090-0241(2006)132:3(388)).
- Park, D.S., Kutter, B.L., 2015. Static and seismic stability of sensitive clay slopes. *Soil Dyn. Earthq. Eng.* 79, 118–129. <https://doi.org/10.1016/j.soildyn.2015.09.006>.
- Phillips, R., Byrne, P., 1998. CANLEX: Modelling slides due to flow liquefaction. *Centrifuge* 98, 627–632.
- Pinatpongsoa, T., Aroonwattanaskul, K., Fang, K., 2020. On the Progression of Slope Failures Using Inverse Velocity of Surface Movements in an Undercut Slope Model. *Workshop on World Landslide Forum*. Springer, 293–301. https://doi.org/10.1007/978-3-030-60706-7_28.
- Porbaha, A., Goodings, D., 1996. Centrifuge modeling of geotextile-reinforced steep clay slopes. *Canadian Geotechnical Journal* 33, 696–704. <https://doi.org/10.1139/t96-096-317>.
- Raisinghani, D., Viswanadham, B., 2011. Centrifuge model study on low permeable slope reinforced by hybrid geosynthetics. *Geotext. Geomembranes* 29 (6), 567–580. <https://doi.org/10.1016/j.geotexmem.2011.07.003>.
- Rajabian, A., Viswanadham, B., Ghiassian, H., Salehzadeh, H., 2012. Centrifuge model studies on anchored geosynthetic slopes for coastal shore protection. *Geotext. Geomembranes* 34, 144–157. <https://doi.org/10.1016/j.geotexmem.2012.06.001>.
- Rajabian, A., Ghiassian, H., Viswanadham, B., 2013. Centrifuge study of anchored geosynthetic slopes. *Geosynthetics International* 20 (3), 191–206. <https://doi.org/10.1680/gein.13.00011>.
- Resnick, G.S., Žnidarčić, D., 1990. Centrifugal modeling of drains for slope stabilization. *Journal of geotechnical engineering* 116 (11), 1607–1624. [https://doi.org/10.1061/\(ASCE\)0733-9410\(1990\)116:11\(1607\)](https://doi.org/10.1061/(ASCE)0733-9410(1990)116:11(1607)).
- Rotte, V.M., Viswanadham, B.V., 2013. Influence of nail inclination and facing material type on soil-nailed slopes. *Proceedings of the Institution of Civil Engineers-Ground Improvement* 166 (2), 86–107. <https://doi.org/10.1680/grim.11.00026>.
- Schofield, A.N., 1980. Cambridge geotechnical centrifuge operations. *Geotechnique* 30 (3), 227–268. <https://doi.org/10.1680/geot.1980.30.3.227>.
- Shen, C., Kim, Y., Bang, S., Mitchell, J., 1982. Centrifuge modeling of lateral earth support. *Journal of the Geotechnical Engineering Division* 108 (9), 1150–1164. <https://doi.org/10.1061/AJGEB6.0001339>.
- Singh, J., Horikoshi, K., Mochida, Y., Takahashi, A., 2019. Centrifugal tests on minimization of flood-induced deformation of levees by steel drainage pipes. *Soils Found.* 59 (2), 367–379. <https://doi.org/10.1016/j.sandf.2018.12.008>.
- Smith, I., Hobbs, R., 1974. Finite element analysis of centrifuged and built-up slopes. *Geotechnique* 24 (4), 531–559. <https://doi.org/10.1680/geot.1974.24.4.531>.
- Sommers, A., Viswanadham, B., 2009. Centrifuge model tests on the behavior of strip footing on geotextile-reinforced slopes. *Geotext. Geomembranes* 27 (6), 497–505. <https://doi.org/10.1016/j.geotexmem.2009.05.002>.
- Song, D., Ng, C.W.W., Choi, C.E., Zhou, G.G., Kwan, J.S., Koo, R., 2017. Influence of debris flow solid fraction on rigid barrier impact. *Canadian geotechnical journal* 54 (10), 1421–1434. <https://doi.org/10.1139/cgj-2016-0502>.
- Song, D., Choi, C.E., Ng, C.W.W., Zhou, G., 2018. Geophysical flows impacting a flexible barrier: effects of solid-fluid interaction. *Landslides* 15 (1), 99–110. <https://doi.org/10.1007/s10346-017-0856-1>.
- Song, D., Choi, C.E., Ng, C.W.W., Zhou, G.G., Kwan, J.S., Sze, H., Zheng, Y., 2019. Load-attenuation mechanisms of flexible barrier subjected to bouldery debris flow impact. *Landslides* 16 (12), 2321–2334. <https://doi.org/10.1007/s10346-019-01243-2>.
- Sonnenberg, R., Bransby, M., Hallett, P., Bengough, A., Mickovski, S., Davies, M., 2010. Centrifuge modelling of soil slopes reinforced with vegetation. *Can. Geotech. J.* 47 (12), 1415–1430. <https://doi.org/10.1139/T10-037>.
- Sonnenberg, R., Bransby, M., Bengough, A., Hallett, P., Davies, M., 2012. Centrifuge modelling of soil slopes containing model plant roots. *Can. Geotech. J.* 49 (1), 1–17. <https://doi.org/10.1139/t11-081>.
- Springman, S., Askarinejad, A., Casini, F., Friedel, S., Kinzler, P., Teyssire, P., Thielen, A., 2012. Lessons learnt from field tests in some potentially unstable slopes in Switzerland. *Acta geotechnica Slovenica* 9, 5–29.
- Sugawara, K.J., Akimoto, M., Kaneko, K., Okamura, H., 1983. Experimental study on rock slope stability by the use of a centrifuge, 5th ISRM Congress.
- Sun, Z., Kong, L., Guo, A., Xu, G., Bai, W., 2019. Experimental and numerical investigations of the seismic response of a rock-soil mixture deposit slope. *Environ. Earth Sci.* 78 (24), 716. <https://doi.org/10.1007/s12665-019-8717-y>.
- Taboada-Urtzuastegui, V., Martinez-Ramirez, G., Abdoun, T., 2002. Centrifuge modeling of seismic behavior of a slope in liquefiable soil. *Soil Dyn. Earthq. Eng.* 22 (9–12), 1043–1049. [https://doi.org/10.1016/S0267-7261\(02\)00129-X](https://doi.org/10.1016/S0267-7261(02)00129-X).
- Takahashi, H., Fujii, N., Sassa, S., 2019. Centrifuge model tests of earthquake-induced submarine landslide. *Int. J. Phys. Model. Geo.*, 1–13 <https://doi.org/10.1680/jphmg.18.00048>.
- Take, W.A., 2015. Thirty-Sixth Canadian Geotechnical Colloquium: Advances in visualization of geotechnical processes through digital image correlation. *Can. Geotech. J.* 52 (9), 1199–1220. <https://doi.org/10.1139/cgj-2014-0080>.
- Take, W.A., Beddoe, R.A., 2014. Base liquefaction: a mechanism for shear-induced failure of loose granular slopes. *Can. Geotech. J.* 51 (5), 496–507. <https://doi.org/10.1139/cgj-2012-0457>.
- Take, W.A., Bolton, M., 2011. Seasonal ratcheting and softening in clay slopes, leading to first-time failure. *Geotechnique* 61 (9), 757–769. <https://doi.org/10.1680/geot.9.P.125>.
- Take, W.A., Bolton, M., Wong, P., Yeung, F., 2004. Evaluation of landslide triggering mechanisms in model fill slopes. *Landslides* 1 (3), 173–184. <https://doi.org/10.1007/s10346-004-0025-1>.
- Take, W.A., Beddoe, R.A., Davoodi-Bilesavar, R., Phillips, R., 2015. Effect of antecedent groundwater conditions on the triggering of static liquefaction landslides. *Landslides* 12 (3), 469–479. <https://doi.org/10.1007/s10346-014-0496-7>.
- Takemura, J., Kimura, T., Hiro-oka, A., Muraishi, H., 1994. Failure of embankment due to seepage flows and its countermeasure. *International conference on centrifuge* 94, 575–580.
- Tamate, S., Suemasa, N., Katada, T., 2012. Simulation of precipitation on centrifuge models of slopes. *International Journal of Physical Modelling in Geotechnics* 12, 89–101. <https://doi.org/10.1680/ijpmg.11.0009>.
- Tamrakar, S., Toyosawa, Y., Itoh, K., Timpong, S., 2006. Failure height comparison during excavation using in-flight excavator, Proceedings of the International Conference on Physical Modeling in Geotechnics-6th ICPMG. 385–390.
- Tang, H., Li, C., Hu, X., Su, A., Wang, L., Wu, Y., Criss, R., Xiong, C., Li, Y., 2015. Evolution characteristics of the Huangtupo landslide based on in situ tunneling

- and monitoring. *Landslides* 12 (3), 511–521. <https://doi.org/10.1007/s10346-014-0500-2>.
- Tang, H., Wasowski, J., Juang, C.H., 2019. Geohazards in the three Gorges Reservoir Area, China—Lessons learned from decades of research. *Eng. Geol.* 105267. <https://doi.org/10.1016/j.enggeo.2019.105267>.
- Taylor, R.N., 1995. *Geotechnical centrifuge technology*. CRC Press.
- Tei, K., TAYLOR, N.R., Milligan, G.W., 1998. Centrifuge model tests of nailed soil slopes. *Soils Found.* 38 (2), 165–177. https://doi.org/10.3208/sandf.38.2_165.
- Thusyanthan, N.I., Madabhushi, S.G., Singh, S., 2006. Centrifuge modeling of solid waste landfill systems—Part 2: Centrifuge testing of model waste. *Geotech. Test. J.* 29 (3), 223–229. <https://doi.org/10.1520/GTJ12299>.
- Thusyanthan, N., Madabhushi, S., Singh, S., 2007. Tension in geomembranes on landfill slopes under static and earthquake loading—Centrifuge study. *Geotext. Geomembranes* 25 (2), 78–95. <https://doi.org/10.1016/j.geotexmem.2006.07.002>.
- Timpong, S., Itoh, K., Toyosawa, Y., 2007. *Geotechnical centrifuge modelling of slope failure induced by ground water table change*. Landslides and Climate Change. London, Taylor and Francis Group, pp. 107–112.
- Turnbull, B., Bowman, E.T., McElwaine, J.N., 2015. Debris flows: experiments and modelling. *Comptes Rendus Physique* 16 (1), 86–96. <https://doi.org/10.1016/j.crhy.2014.11.006>.
- Vallejo, L., Estrada, N., Taboada, A., Caicedo, B., Silva, J., 2006. Numerical and physical modeling of granular flow. *Physical Modelling in Geotechnics*. Taylor & Francis, Milton Park.
- Veenhof, R., Wu, W., 2018. Root Reinforcement to Stabilize Slopes, Proceedings of China-Europe Conference on Geotechnical Engineering. Springer, pp. 1320–1323.
- Viswanadham, B., Mahajan, R., 2007. Centrifuge model tests on geotextile-reinforced slopes. *Geosynthetics International* 14 (6), 365–379. <https://doi.org/10.1680/gein.2007.14.6.365>.
- Vorster, P., Gräbe, P., Jacobsz, S.W., 2017. Centrifuge modelling of railway embankments under static and cyclic loading. *J. S. Afr. Inst. Civ. Eng.* 59 (3), 2–10. <https://doi.org/10.17159/2309-8775/2017/v59n3a1>.
- Wang, S., Idinger, G., Wu, W., 2021. Centrifuge modelling of rainfall-induced slope failure in variably saturated soil. *Acta Geotechnica* 16, 2899–2916. <https://doi.org/10.1007/s11440-021-01169-x>.
- Wang, G., Sassa, K., 2003. Pore-pressure generation and movement of rainfall-induced landslides: effects of grain size and fine-particle content. *Eng. Geol.* 69 (1–2), 109–125. [https://doi.org/10.1016/S0013-7952\(02\)00268-5](https://doi.org/10.1016/S0013-7952(02)00268-5).
- Wang, L., Zhang, G., Zhang, J.M., 2010a. Nail reinforcement mechanism of cohesive soil slopes under earthquake conditions. *Soils Found.* 50 (4), 459–469.
- Wang, R., Zhang, G., Zhang, J.-M., 2010b. Centrifuge modelling of clay slope with montmorillonite weak layer under rainfall conditions. *Applied Clay Science* 50 (3), 386–394.
- Wang, L.P., Zhang, G., 2014. Centrifuge model test study on pile reinforcement behavior of cohesive soil slopes under earthquake conditions. *Landslides* 11 (2), 213–223. <https://doi.org/10.1007/s10346-013-0388-2>.
- Wang, Y., Zhang, G., Wang, A., 2018a. Block reinforcement behavior and mechanism of soil slopes. *Acta Geotechnica* 13 (5), 1155–1170.
- Wang, Y., Zhang, G., Wang, A., 2018b. On the cyclic failure mechanism of soil slopes. *Acta Geotechnica* 13 (6), 1419–1432.
- Wieczorek, G.F., 1996. Landslides: investigation and mitigation. Chapter 4—Landslide triggering mechanisms. Transportation Research Board Special Report (247).
- Wolinsky, E., Take, W.A., 2019. Instability of loose dry granular slopes observed in centrifuge tilting table tests. *Géotechnique Letters* 9 (2), 147–153. <https://doi.org/10.1680/jgele.19.00015>.
- Xu, J., Ueda, K., Uzuoka, R., 2022. Evaluation of failure of slopes with shaking-induced cracks in response to rainfall. *Landslides*, 1–18. <https://doi.org/10.1007/s10346-021-01734-1>.
- Yan, K., Zhang, J., Cheng, Q., Wu, J., Wang, Z., Tian, H., 2019. Earthquake loading response of a slope with an inclined weak intercalated layer using centrifuge modeling. *B. Eng. Geol. Environ.* 78 (6), 4439–4450. <https://doi.org/10.1007/s10064-018-1421-4>.
- Yao, W., Li, C., Zhan, H., Zhou, J.-Q., Criss, R.E., Xiong, S., Jiang, X., 2020. Multiscale Study of Physical and Mechanical Properties of Sandstone in Three Gorges Reservoir Region Subjected to Cyclic Wetting-Drying of Yangtze River Water. *Rock Mech. Rock Eng.*, 1–17 <https://doi.org/10.1007/s00603-019-02037-7>.
- Yin, M., Rui, Y., Xue, Y., 2019. Centrifuge study on the runout distance of submarine debris flows. *Mar. Georesour. Geotech.* 37 (3), 301–311. <https://doi.org/10.1080/1064119X.2017.1411407>.
- Yoon, B., Ellis, E., 2009. Centrifuge modelling of slope stabilisation using a discrete pile row. *Geomechanics and Geoengineering: An International Journal* 4 (2), 103–108. <https://doi.org/10.1080/17486020902856991>.
- Yu, Y., Deng, L., Sun, X., Lu, H., 2008. Centrifuge modeling of a dry sandy slope response to earthquake loading. *B. Earthq. Eng.* 6 (3), 447–461. <https://doi.org/10.1007/s10518-008-9070-9>.
- Yu, Y.Z., Deng, L.J., Sun, X., Lü, H., 2010. Centrifuge modeling of dynamic behavior of pile-reinforced slopes during earthquakes. *J. Cent. South Univ. Technol.* 17 (5), 1070–1078. <https://doi.org/10.1007/s11771-010-0599-9>.
- Zhang, W., Askarinejad, A., 2019. Centrifuge modelling of submarine landslides due to static liquefaction. *Landslides* 16 (10), 1921–1938. <https://doi.org/10.1007/s10346-019-01200-z>.
- Zhang, G., Wang, L., 2016. Integrated analysis of a coupled mechanism for the failure processes of pile-reinforced slopes. *Acta Geotechnica* 11 (4), 941–952. <https://doi.org/10.1007/s11440-015-0410-z>.
- Zhang, G., Wang, L., 2017. Simplified evaluation on the stability level of pile-reinforced slopes. *Soils Found.* 57 (4), 575–586. <https://doi.org/10.1016/j.sandf.2017.03.009>.
- Zhang, G., Hu, Y., Zhang, J.M., 2009. New image analysis-based displacement-measurement system for geotechnical centrifuge modeling tests. *Measurement* 42 (1), 87–96. <https://doi.org/10.1016/j.measurement.2008.04.002>.
- Zhang, G., Wang, R., Qian, J., Zhang, J.M., Qian, J., 2012. Effect study of cracks on behavior of soil slope under rainfall conditions. *Soils Found.* 52 (4), 634–643. <https://doi.org/10.1016/j.sandf.2012.07.005>.
- Zhang, G., Cao, J., Wang, L., 2013. Centrifuge model tests of deformation and failure of nailing-reinforced slope under vertical surface loading conditions. *Soils Found.* 53 (1), 117–129. <https://doi.org/10.1016/j.sandf.2012.12.008>.
- Zhang, H., Chen, C., Zheng, Y., Yu, Q., Zhang, W., 2020a. Centrifuge modeling of layered rock slopes susceptible to block-flexure toppling failure. *B. Eng. Geol. Environ.*, 1–17.
- Zhang, C., Cai, Z.Y., Huang, Y.H., Chen, H., 2018. Laboratory and Centrifuge Model Tests on Influence of Swelling Rock with Drying-Wetting Cycles on Stability of Canal Slope. *Advances in Civil Engineering*: 4785960.
- Zhang, G., Li, M., Wang, L., 2014. Analysis of the effect of the loading path on the failure behaviour of slopes. *KSCE J. Civ. Eng.* 18 (7), 2080–2084. <https://doi.org/10.1007/s12205-014-1461-7>.
- Zhang, G., Hu, Y., Wang, L., 2015b. Behaviour and mechanism of failure process of soil slopes. *Environ. Earth Sci.* 73 (4), 1701–1713.
- Zhang, Bei, Huang, Yu, 2022. Impact behavior of superspeed granular flow: Insights from centrifuge modeling and DEM simulation. *Eng. Geol.* 299, 106569. <https://doi.org/10.1016/j.enggeo.2022.106569>.
- Zhang, L., Li, J., Li, X., Zhang, J., Zhu, H., 2018b. *Rainfall-induced soil slope failure: stability analysis and probabilistic assessment*. CRC Press.
- Zhang, X., Lu, X., Shi, Y., Xia, Z., Liu, W., 2015c. Centrifuge experimental study on instability of seabed stratum caused by gas hydrate dissociation. *Ocean Eng.* 105, 1–9.
- Zhang, J.M., Luo, Y., Zhou, Z., Chong, L., Victor, C., Zhang, Y.F., 2021. Effects of preferential flow induced by desiccation cracks on the slope stability. *Engineering Geology* 106164. <https://doi.org/10.1016/j.enggeo.2021.106164>.
- Zhang, S., Pei, X., Wang, S., Huang, R., Zhang, X., Chang, Z., 2019a. Centrifuge model testing of a loess landslide induced by rising groundwater in Northwest China. *Eng. Geol.* 259, 105170.
- Zhang, S., Pei, X., Wang, S., Huang, R., Zhang, X., 2020b. Centrifuge Model Testing of Loess Landslides Induced by Excavation in Northwest China. *Int. J. Geomech.* 20 (4), 04020022.
- Zhang, J., Pu, J., Zhang, M., Qiu, T., 2001. Model tests by centrifuge of soil nail reinforcements. *Journal of testing and evaluation* 29 (4), 315–328. <https://doi.org/10.1520/JTE12261>.
- Zhang, J., Chen, Z., Wang, X., 2007. Centrifuge modeling of rock slopes susceptible to block toppling. *Rock Mech. Rock Eng.* 40 (4), 363–382. <https://doi.org/10.1007/s00603-006-0112-9>.
- Zhang, J., Lin, H., Wang, K., 2015a. Centrifuge modeling and analysis of submarine landslides triggered by elevated pore pressure. *Ocean Engineering* 109, 419–429.
- Zhang, L., Shi, B., Zeni, L., Minardo, A., Zhu, H., Jia, L., 2019b. An fiber Bragg grating-based monitoring system for slope deformation studies in geotechnical centrifuges. *Sensors* 19, 1591.
- Zhang, Z., Wang, T., Wu, S., Tang, H., Liang, C., 2017. Investigation of dormant landslides in earthquake conditions using a physical model. *Landslides* 14 (3), 1181–1193. <https://doi.org/10.1007/s10346-017-0813-z>.
- Zhang, M., Wu, H., 2007. Rainfall simulation techniques in centrifuge modelling of slopes. *Rock and Soil Mechanics* 28, 53–57. <https://doi.org/10.16285/j.rsm.2007.s1.084>, in Chinese.
- Zhao, X., Salgado, R., Prezzi, M., 2014. Centrifuge modelling of combined anchors for slope stability. *Proceedings of the Institution of Civil Engineers-Geotechnical Engineering* 167 (4), 357–370. <https://doi.org/10.1680/geng.12.00076>.
- Zhao, Y., Zhang, G., Hu, D., Han, Y., 2018. Centrifuge Model Test Study on Failure Behavior of Soil Slopes Overlying the Bedrock. *Int. J. Geomech.* 18 (11), 04018144. [https://doi.org/10.1061/\(ASCE\)GM.1943-5622.0001292](https://doi.org/10.1061/(ASCE)GM.1943-5622.0001292).
- Zhen, F., Yueping, Y., Bin, L., Jinkai, Y., 2013. Physical Modeling of Landslide Mechanism in Oblique Thick-Bedded Rock Slope: A Case Study. *Acta Geologica Sinica-English Edition* 87 (4), 1129–1136. <https://doi.org/10.1111/1755-6724.12115>.
- Zhou, R., Ng, C., Zhang, M., Pun, W., Shiu, Y., Chang, G., 2006. The effects of soil nails in a dense steep slope subjected to rising groundwater, Proceedings of the Sixth International Conference on Physical Modelling in Geotechnics, Hong Kong, pp. 397–405.
- Zhou, Y.G., Meng, D., Ma, Q., Huang, B., Ling, D.S., Chen, Y.M., 2019. Centrifuge modeling of dynamic response of high fill slope by using generalized scaling law. *Eng. Geol.* 260, 105213. <https://doi.org/10.1016/j.enggeo.2019.105213>.

- Zhu, C., He, M., Karakus, M., Cui, X., Tao, Z., 2020. Investigating toppling failure mechanism of anti-dip layered slope due to excavation by physical modelling. *Rock Mechanics and Rock Engineering* 53, 5029–5050. <https://doi.org/10.1007/s00603-020-02207-y>.
- Zimmie, T., Pamuk, A., Adalier, K., Mahmud, M., 2005. Retrofit-reinforcement of cohesive soil slopes using high strength geotextiles with drainage capability. *Geotech. Geol. Eng.* 23 (4), 447–459. <https://doi.org/10.1007/s10706-004-9113-1>.
- Zornberg, J.G., Mitchell, J., Sitar, N., 1997. Testing of reinforced slopes in a geotechnical centrifuge. *Geotech. Test. J.* 20 (4), 470–480. <https://doi.org/10.1520/GTJ10413j>.
- Zornberg, J.G., Sitar, N., Mitchell, J.K., 1998. Performance of geosynthetic reinforced slopes at failure. *J. Geotech. Geoenviron.* 124 (8), 670–683. [https://doi.org/10.1061/\(ASCE\)1090-0241\(1998\)124:8\(670\)](https://doi.org/10.1061/(ASCE)1090-0241(1998)124:8(670)).